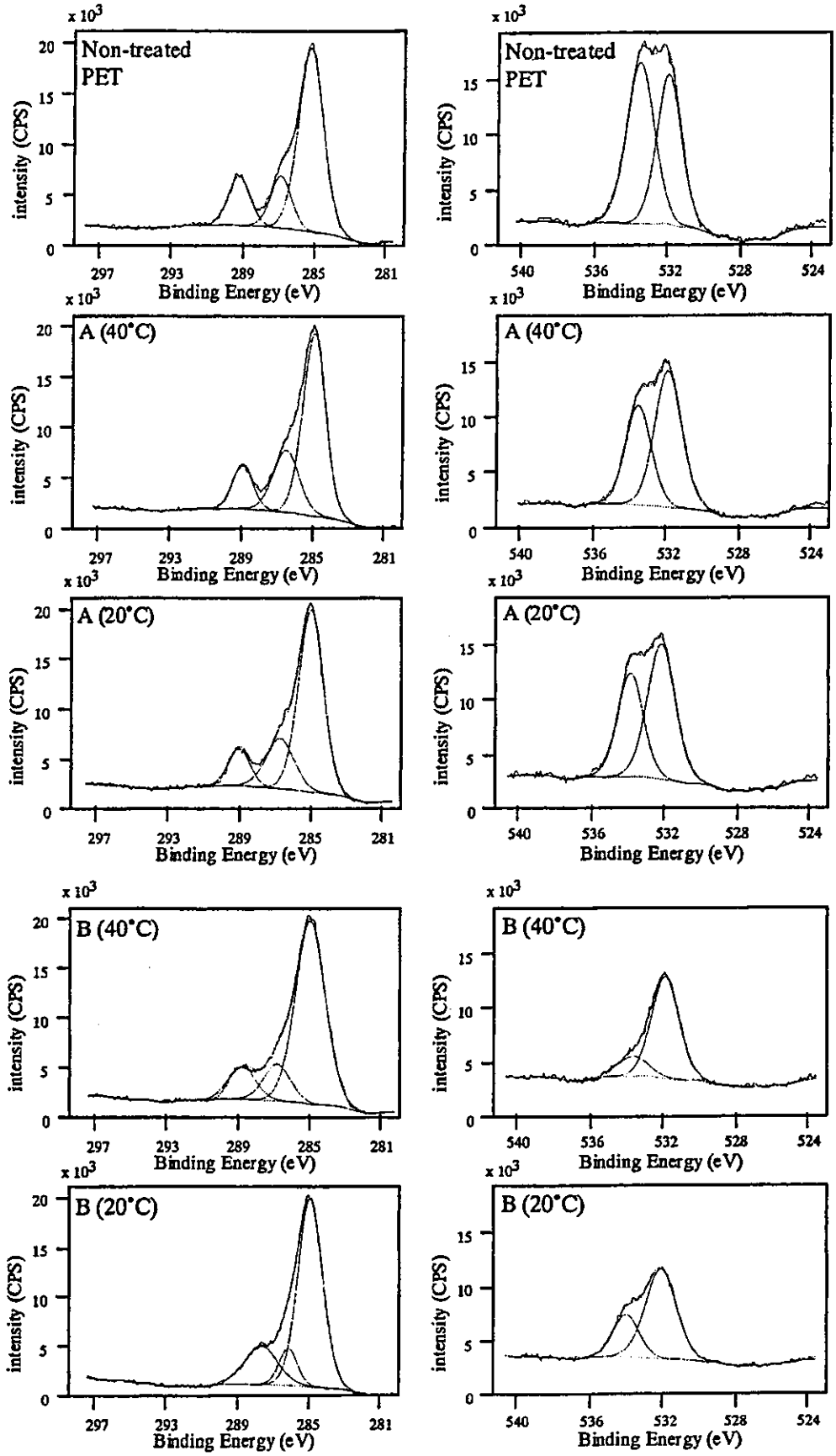

Figure 3. High-resolution C_{1S} and O_{1S} spectra of PNIPAM–heparin-adsorbed and -desorbed PET surfaces: (A) nontreated PET and (B) treated with PNIPAM–heparin with a graft chain mol wt of 2×10^3 g/mol.

Table 2. Temperature Dependence of Wettability and Surface Chemical Composition at Adsorption and Washing Steps on the PET Surface[a]

sample	temperature (°C)		water contact angle (deg)		elemental ratio	
	adsorption	washing	advancing	receding	O/C	N/C
nontreated PET			59.0 ± 1.8	41.8 ± 1.9	0.34 (0.40)	
c1	20	20	65.8 ± 4.0	33.5 ± 2.9	0.22	0.06
c2	40	20	64.5 ± 4.5	32.7 ± 1.6	0.20	0.09
c3	40	40	52.5 ± 11.5	13.7 ± 5.3	0.17	0.10
PNIPAM	40	40	49.2 ± 10.0	10.8 ± 1.5	0.12 (0.17)	0.15 (0.17)

[a] PNIPAM–heparin with a PNIPAM graft chain mol wt of 1×10^5 g/mol was used.

Table 3. Amount of Adsorbed PNIPAM–Heparin before and after Washing at 40 and 20 °C ($n = 3$)

fluorescence-labeled PNIPAM–heparin (mol wt of PNIPAM chain, g/mol)	amount of coating (μg/mm^2)	remaining PNIPAM–heparin (μg/mm^2) after washing		percent of remaining amount after washing (%)	
		20 °C	40 °C	20 °C	40 °C
2×10^3	2.40 ± 0.15	0.87 ± 0.06	1.28 ± 0.03	36.4	53.4
1×10^4	2.62 ± 0.08	1.11 ± 0.01	1.61 ± 0.03	42.8	61.8
1×10^5	2.60 ± 0.30	2.00 ± 0.06	2.36 ± 0.20	76.4	90.1

Table 4. Temperature Dependence of Wettability and Surface Chemical Composition at Adsorption and Washing Steps on PST and PU Surfaces[a]

material	mol wt of PNIPAM chain($\times 10^4$ g/mol)	water contact angle (deg) (washing temperature)				elemental ratio (washing temperature)			
		20 °C		40 °C		20 °C		40 °C	
		advancing	receding	advancing	receding	N/C	O/C	N/C	O/C
PS	nontreated	85.9 ± 1.2	85.5 ± 1.4	79.5 ± 0.8	81.1 ± 1.3	0.00	0.01		
	0.2	67.7 ± 1.6	30.0 ± 1.1	64.2 ± 2.9	32.6 ± 10.7	0.03	0.07	0.02	0.04
	1.0	63.3 ± 0.4	37.2 ± 1.6	66.1 ± 3.6	20.4 ± 10.7	0.05	0.10	0.08	0.12
	10.0	39.0 ± 5.4	15.9 ± 9.5	46.0 ± 12.8	12.5 ± 1.8	0.10	0.14	0.11	0.14
PU	nontreated	73.0 ± 1.6	49.7 ± 0.7	73.4 ± 1.7	44.9 ± 1.7	0.03	0.26		
	0.2	68.3 ± 2.4	45.1 ± 1.4	70.3 ± 2.3	42.9 ± 1.6	0.03	0.33	0.03	0.27
	1.0	76.1 ± 4.1	45.7 ± 1.8	26.5 ± 4.1	<10	0.04	0.26	0.13	0.18
	10.0	72.7 ± 3.5	41.0 ± 4.1	22.3 ± 9.6	<10	0.04	0.25	0.11	0.20

[a] PNIPAM–heparin samples with different mol wt graft chains were used.

The amounts of adsorbed PNIPAM–heparin, which were determined using fluorescence-labeled PNIPAM–heparin in which the hydroxyl group was partially derivatized with a fluorescent dye (DTAF) according to our method previously reported[12] using the CSLM, were as follows: A fixed amount (2.60 μg/nm^2) of PNIPAM–heparin with a PNIPAM mol wt of 2×10^3 and 1×10^5 was coated on PET films. After being air-dried, the films were subjected to immersion into water at 20 or 40 °C for 6 h, and subsequently the surface fluorescence was scanned under the CLSM. Table 3 lists the remaining amount of PNIPAM–heparin with different mol wt graft chains, which was calculated from the predetermined standard linear relations between the amount of fluorescence-labeled PNIPAM–heparin and fluorescence intensity. At 40 °C, a larger amount of remaining PNIPAM–heparin was observed for PNIPAM–heparin with the highest mol wt (2×10^3), followed by PNIPAM–heparin with an intermediate mol wt of PNIPAM (1×10^4). The lowest adsorption amount at 40 °C and highest desorption amount was found for PNIPAM–gelatin with a lower mol wt (2×10^3). Table 3 also lists the percentage of remaining amount of PNIPAM–heparin upon washing at 40 or 20 °C: a higher mol wt of PNIPAM leads to higher adsorption at 40 °C and low desorption at 20 °C. A lower mol wt of PNIPAM–heparin apparently desorbed considerably at 20 °C.

Substrate Dependency on Adsorptivity/Desorptivity. It is of interest to know whether such thermoresponsiveness of adsorption and desorption depends on the type of substrate films. To this end, substrate dependency of thermoresponsiveness of adsorption and desorption of PNIPAM–heparin was carried out as follows. In addition to PET as mentioned above, two polymeric films (PST and PU) were studied. Table 4 lists surface chemical compositions (determined by XPS) and wettabilities (determined by advancing and receding contact angles). Irrespective of the type of polymer films, the general tendency is as follows: (1) An increase in the mol wt of the PNIPAM chain appears to increase the N/C ratio but to reduce the O/C ratio, irrespective of temperature. A marked increase in the N/C ratio was observed for the highest mol wt of PNIPAM. (2) In general, the N/C ratio at 40 °C was higher than that at 20 °C. Since the nitrogen atom is mainly derived from the PNIPAM molecule, an increase in the N/C ratio means that PNIPAM–heparin adsorbs well on the polymer surface at 40 °C. High-resolution C_{1S} spectra of samples before and after coating/washing provide more detailed information on adsorption and desorption characteristics, as shown in Figures 4 and 5. For PST, with an increase in the mol wt of the graft chain, the relative intensity fraction of carbonyl carbon in the C_{1S} spectra of both PST and PU films, both of which were subjected to washing at 40 °C, was increased. However, upon washing at 20 °C, a considerably large fraction of carbonyl carbon disappeared in the spectra of both films, irrespective of the mol wt of the graft chain, except for PST coated with PNIPAM–heparin with the highest mol wt graft chain; there is little difference in the fine structure of the C_{1S} spectra and wettability between 20 and 40 °C (Table 4). From XPS and wettability measurements, it can be said that the desorption was easier for PET and PU as compared with PST.

Complexation with ATIII. It is of primary importance to determine whether PNIPAM–heparin adsorbed on surfaces can be complexed with ATIII since the antithrombin activity of ATIII is markedly increased by complexation with heparin. After the PET films were

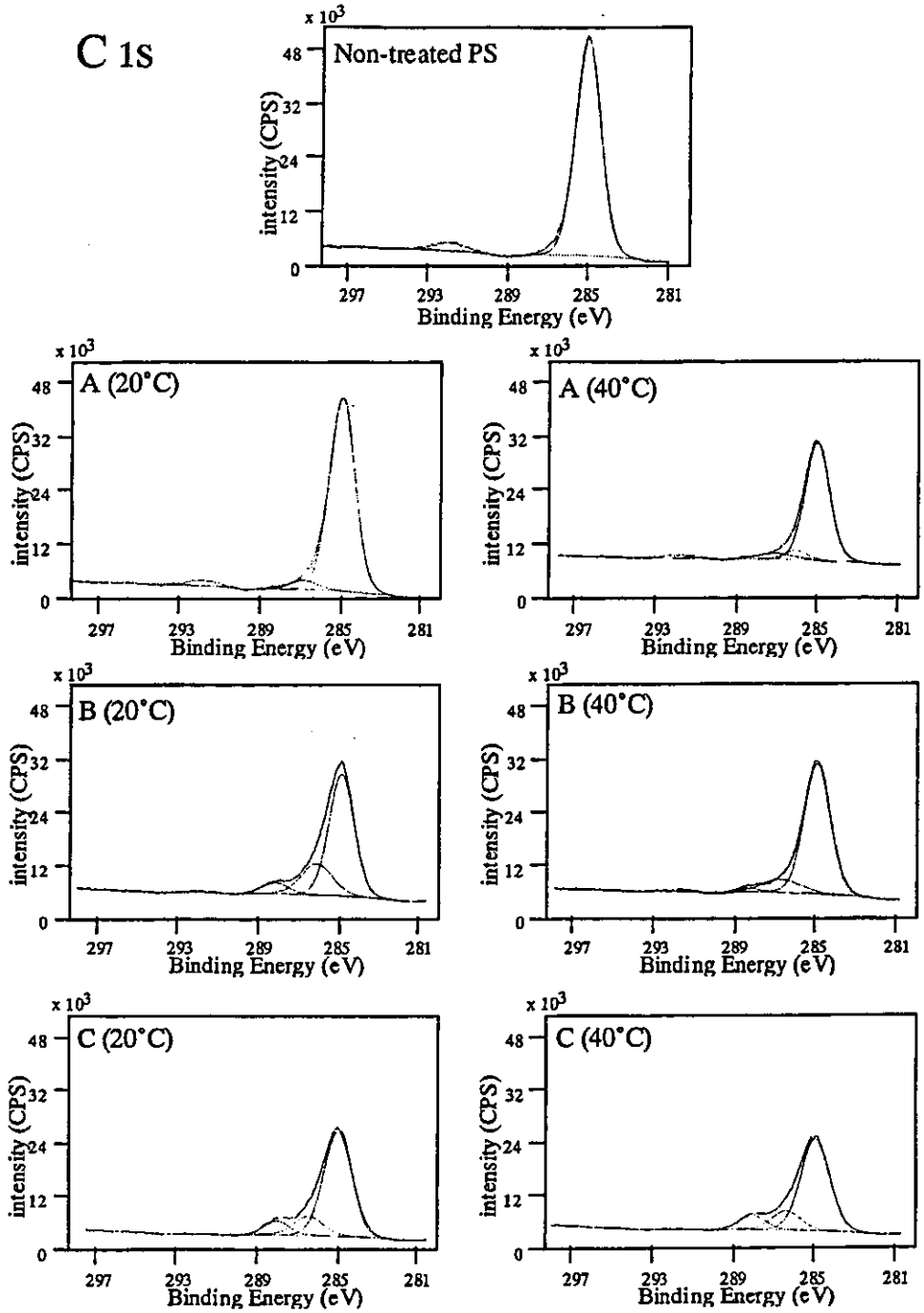

Figure 4. High-resolution C_{1S} spectra of polystyrene films with or without treatments of adsorption/desorption of PNIPAM–heparin with different mol wt graft chains. The mol wt of graft chains: (A) 2×10^3 g/mol, (B) 1×10^4 g/mol, and (C) 1×10^5 g/mol. Temperature denotes the washing temperature.

immersed in a 1% aqueous solution containing PNIPAM–heparin and dried, the films were washed with water at 40 °C. Subsequently, the films were immersed in an albumin-containing buffer solution for 1 h and immersed in an ATIII-containing buffer solution according to the instructions on the use of the ABC (avidin–biotinylated enzyme complex) kit; immunostaining was carried out by sequential treatment using an anti-ATIII antibody, biotinylated IgG, and avidin-coupled alkaline phosphatase and final staining using a chromogenic substrate. All of these steps were carried out at 40 °C. Figure 6A shows the fluorescence intensity dependence on the mol wt of PNIPAM, which was determined using the CLSM. Figure 6B strongly indicates that the relative fluorescence intensity (nontreated PET film was used as a control) increased significantly with an increase in the mol wt of the PNIPAM chain, indicating that high-mol-wt PNIPAM–heparin has a much greater capacity for complexation with ATIII than low-mol-wt PNIPAM–heparin.

Temperature-Dependent Adsorption/Desorption and Complexation with ATIII. The temperature dependency of coating and washing steps upon adsorption and desorption of PNIPAM–heparin and its ATIII complexation was determined as follows. The PET films were

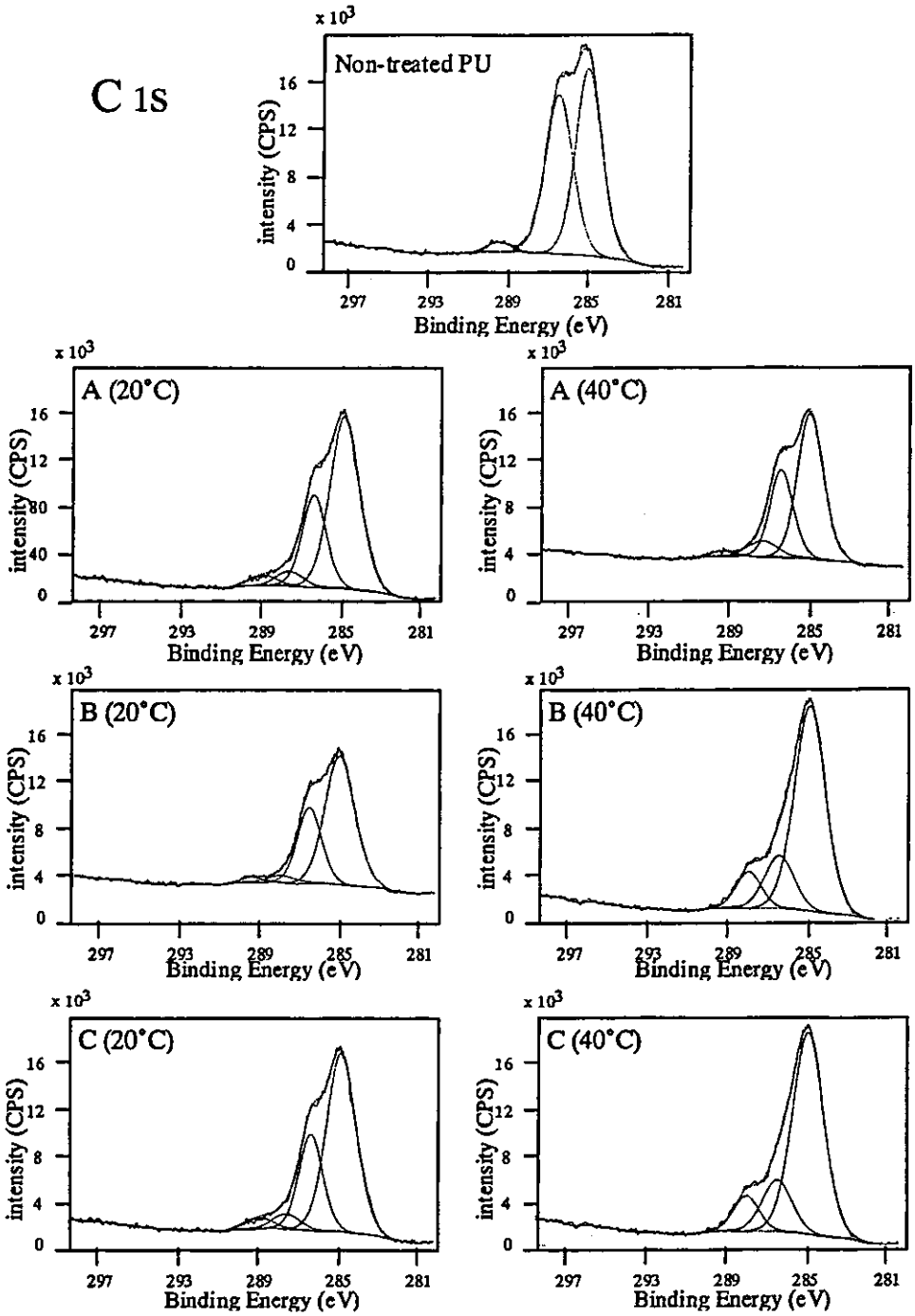

Figure 5. High-resolution C_{1S} spectra of segmented polyurethane with or without treatments of adsorption/desorption of PNIPAM–heparin with different mol wt of graft chains. The mol wt of graft chain; A (2×10^3 g/mol), B (1×10^4 g/mol), and C (1×10^5). Temperature denotes the washing temperature.

immersed in a 1% aqueous solution containing PNIPAM–heparin and incubated at either 20 or 40 °C for 30 min (adsorption step) and then subjected to washing with water at either 20 or 40 °C. The wettability and XPS measurements showed that adsorption of PNIPAM–heparin is enhanced at treatment temperatures above LCST (Table 3). That is, when the temperature at both the adsorption and washing steps was 20 °C, only a slight decrease in receding contact angle, a reduced O/C ratio, and an increased N/C ratio were observed. This is the same in the case of the adsorption temperature of 40 °C and washing temperature of 20 °C, indicating that adsorbed PNIPAM–heparins were removed from the surface although some of them remained. On the other hand, a markedly reduced receding angle, a decreased O/C ratio, and an increased N/C ratio, the last two of which approached the theoretical values of PNIPAM, were noted when the temperature at both steps was 40 °C. Therefore, it can be said that at a physiological temperature, PNIPAM–heparin is precipitated and remains on the surface.

Fluorescent images of samples subjected to adsorption and desorption (each step was carried out at 20 or 40 °C) were obtained as follows: first, immersion into albumin-

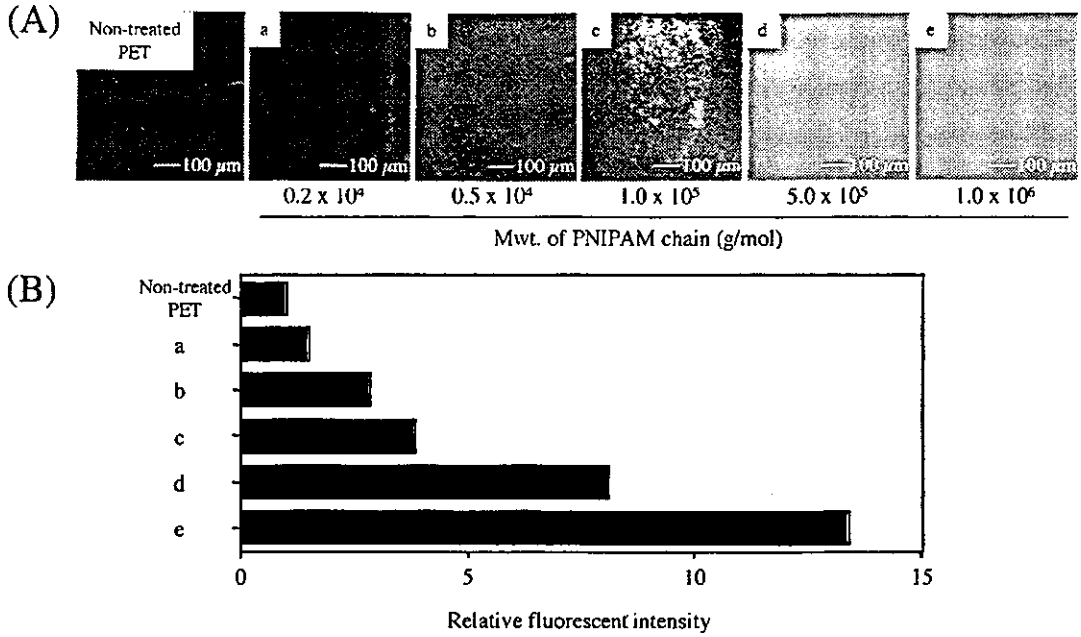

Figure 6. Complexation of PNIPAM–heparin with ATIII. (A) Fluorescence images measured by the CLSM, as a function of the mol wt of the PNIPAM chain in PNIPAM–heparin (after treatment with albumin as a blocking agent followed by ATIII, chromogenic staining using an ABC kit was performed). (B) The relative fluorescence intensity as a function of the mol wt of the PNIPAM chain in PNIPAM–heparin (the fluorescence intensity of the nontreated PET film is used as a control).

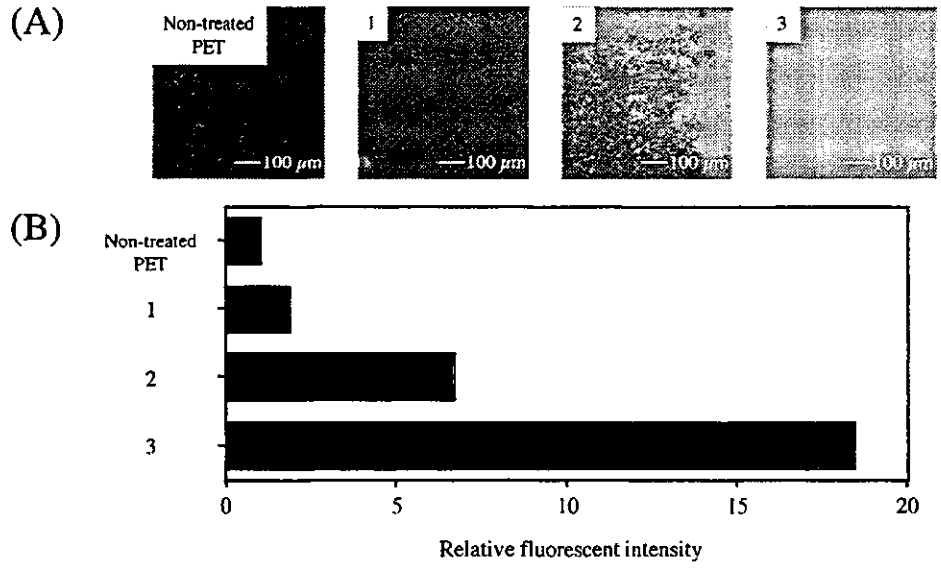

Figure 7. ATIII complexation capacity vs treatment temperature (mol wt of PNIPAM chain in PNIPAM–heparin: 1×10^4). The PET film, which is immersed in an aqueous solution containing PNIPAM–heparin, was incubated at either 20 or 40 °C (adsorption temperature) and then washed with water at either 20 or 40 °C (desorption temperature). Prior to adsorption of ATIII and ABC-kit treatment, albumin blocking treatment was performed. Adsorption and desorption temperatures are 20 and 20 °C for c1, 40 and 20 °C for c2, and 40 and 40 °C for c3, respectively. (c1, c2, c3 are referred to Table 2.)

containing buffer solution for blocking to avoid undesirable adsorption of proteins used for following successive procedures, subsequent immersion into the ATIII-containing buffer solution, and then treatment using the ABC kit as described above, as shown in Figure 7A. Note that the fluorescence intensities for nontreated PET film and the ATIII-free sample were very small. When the temperature for both adsorption and desorption was 20 °C, only a slight increase in the fluorescence intensity was noted as compared with the nontreated PET film surface as a control, whereas in the case of the adsorption temperature of 20 °C and desorption temperature of 40 °C, an almost 6-fold increase in the fluorescence intensity was noted (Figure 7B). When the temperature at both steps was 40 °C, a very high fluorescence intensity (almost 18 times higher than that of the control) was observed. Such film was also incubated in serum-containing medium (DMEM with 10% FCS) for 1 h. There was little difference in the fluorescence intensity before and after incubation. These results strongly indicate that the amount of adsorbed PNIPAM–heparin mainly depends on the temperature at the treatment steps; that is, when the treatment temperature was lower than LCST, desorption of PNIPAM–heparin was predominant, and when the temperature was higher than LCST, very high stability even in the serum-containing medium was noticed.

Discussion

Thermoresponsive polymer systems with LCST of approximately the physiological temperature range have received considerable attention in the biomedical field where the temperature-induced sol-to-gel transformation or phase transition phenomenon plays a significant role in biomedical functioning.[19] For example, thermoresponsive polymeric systems have been used in drug delivery matrixes,[20] cell sheet detachable two-dimensional (2D) cell substrate matrixes,[21,22] and three-dimensional (3D) cell-entrapping artificial extracellular matrixes[23,24] for tissue-engineering devices, in wound-healing matrixes for hemostasis,[25] and as tissue adhesion prevention material.[19] These are realized by utilizing a thermoresponsive physical phase transformation such as sol-to-gel or gel-to-sol transformations, depending on the type of application.

Thermoresponsiveness has been induced by incorporating a polymeric unit with LCST at an approximately physiological temperature into a designed material. To this end, the NIPAM monomer unit has been often used since the LCST of PNIPAM is approximately 32 °C. The present study showed that PNIPAM-conjugated heparin exhibited a thermoresponsive behavior such as solubilization or precipitation in the aqueous phase and adsorption or desorption at the water/substrate interface. Behavioral control would require precise control of the mol wt of PNIPAM, as indicated in this study. That is, complete precipitation above LCST in an aqueous solution and a strong adsorption characteristic were attained with higher-mol-wt PNIPAM (Figure 1). Control of the mol wt of PNIPAM was realized by iniferter photopolymerization, which was originally developed by Otsu et al. in the early 1980s.[14] The unique feature of this iniferter photopolymerization is that it proceeds in a quasi-living polymerization manner, in which "active" and "dormant" propagating chain ends are reversibly equilibrated under UV irradiation. This enables minimal transfer or termination reactions if an appropriate reaction condition is well selected. In our previous studies,[16-20] we developed iniferter-based graft-polymerized surfaces and block copolymers as surface coatings, both of which were designed to realize biocompatible surfaces.

Using this technique, we synthesized heparin with an iniferter group at its terminus under defined mild conditions without substantial cleavage of backbone and side chains and initiated living polymerization of NIPAM as schematically shown in Scheme 1. The resultant PNIPAM–heparin has LCST in an aqueous solution. LCST and complete or partial precipitation above LCST depended on the mol wt of PNIPAM: an increase in the mol wt of the graft chain lowered LCST. The stability of adsorbed PNIPAM–heparin on polymer films was higher at 40 °C than at 20 °C as evidenced by its wettability and surface chemical compositions (Figures 2–5). Although there was a small wettability difference with an increase in the mol wt of PNIPAM (Figure 2A), the surface coverage estimated from the surface chemical composition (Figure 2B) was enhanced with a higher mol wt of PNIPAM. The high-resolution analysis of subpopulations of C_{1s} and O_{1s} spectra clearly demonstrated the thermoresponsive adsorption and desorption and its graft chain mol wt dependency and substrate dependency (Figures 2–5). A higher mol wt graft chain and a highly hydrophobic surface such as PST enhanced surface adsorption at 40 °C and reduced desorption at 20 °C. These results indicate that a hydrophobic interaction-driven process is dominant. In fact, for hydrophobic PST, there appears little desorption at 20 °C when PNIPAM–heparin with a high mol wt graft chain is employed (Figure 4 and Table 3).

The degree of complexation with ATIII, which determines the degree of anticoagulation, was also significantly enhanced with a higher mol wt of PNIPAM (Figure 3). This means that higher-mol-wt PNIPAM enhances the adsorption of heparin (higher adsorption capability and less desorption capability than those of lower-mol-wt PNIPAM).

In addition to the amount of PNIPAM–heparin adsorbed on the film surface, the configuration of PNIPAM–heparin is also considered as a determinant of anticoagulation activity: the ideal configuration is that the PNIPAM segment is anchored on the surface and the heparin molecule is oriented vertically in the aqueous phase, thus facilitating complexation with ATIII at a physiological temperature. This configuration is best suited for surface heparinization without substantial loss of the biological activity of heparin, as proposed and verified by Olsson's end-point attachment of the heparin molecule via the surface-coupling approach,[7] our alkylated heparin as a heparin surfactant via the surface adsorption approach,[12] and the biomimetic engineered glycolyx-like surface approach using oligosaccharide surfactant polymers developed by Marchant et al.[26] Marchant's oligosaccharide surfactant polymers consisted of flexible poly(vinylamine) with dextran and alkanoyl side chains. They demonstrated that alkanoyl side groups self-assemble on the hydrophobic surface via epitaxial adsorption, the main chains lie parallel to the surface, and solvated oligosaccharide side chains protrude into the aqueous phase, creating a glycocalyx-like coating. The resulting biomimetic surface is effective in suppressing protein adsorption and adhesion.

Taken together with this evidence, it can be said that bioconjugation of bioactive heparin and PNIPAM having a thermally induced phase transition characteristic provides a thermoresponsive surface biocompatible coating via adsorption and precipitation. Although we have not evaluated the anticoagulant activity of PNIPAM–heparin as a thermoresponsive biocompatible coating on an extracorporeal circuit, treatment of the entire blood-contacting surface of a device with an aqueous solution containing with PNIPAM–heparin at room temperature and subsequent elevation of temperature to a physiological temperature may provide a heparinized surface on which the heparin molecule is exposed to the fluid phase and the precipitated PNIPAM segment is anchored on the surface of the extracorporeal device, which appears to resist replacement with hydrophobic plasma components. In fact, the incubation of PNIPAM–heparin-treated film in the serum-containing medium did not induce the significant change in surface biological activity as mentioned above; this results in the maintenance of antithrombogenicity at least for a short-term extracorporeal circulation.

(18) Kidoaki, S.; Nakayama, H.; Matsuda, T. *Langmuir* **2001**, *17*, 1080–1087.
(19) Ohya, S.; Nakayama, Y.; Matsuda, T. *Biomacromolecules* **2001**, *2*, 856–863.
(20) Miura, M.; Cole, C.-A.; Monji, N.; Hoffman, A. S. *J. Biomater. Sci., Polym. Ed.* **1994**, *5*, 555–568.
(21) Takezawa, T.; Yamazaki, M.; Mori, Y.; Yonaha, T.; Yoshizato, K. *J. Cell Sci.* **1992**, *101*, 495–501.
(22) Okano, T.; Yamada, N.; Sakai, H.; Sakurai, Y. *J. Biomed. Mater. Res.* **1993**, *27*, 1243–1251.
(23) Matsuda, T.; Moghaddam, M. J. *Mater. Sci. Eng.* **1993**, *C1*, 37–43.
(24) Moghaddam, M. J.; Matsuda, T. *ASAIO Trans.* **1991**, *37*, 437–438.
(25) Morikawa, N.; Matsuda, T. J. *Biomat. Sci.*, in press.
(26) Holland, N. B.; Qui, Y.; Ruegsegger, M.; Marchant, R. E. *Nature* **1998**, *39*, 799–801.

In conclusion, PNIPAM−heparin is a thermoresponsive biocompatible coating material. The adsorption and stability of adsorbed PNIPAM−heparin were enhanced with an increase in the mol wt of PNIPAM. Simultaneously, complexation of heparin with ATIII was enhanced. Desorption was facilitated by decreasing the temperature of water and by using polar surfaces such as PET and PU. We have not yet investigated how such a temperature-induced "switching on and off" of anticoagulant activity functions well in vivo, but we are planning to verify such biofunctioning using a minicolumn simulating extracorporeal circulatory device. Thus, it can be concluded that the combination of thermoresponsive PNIPAM and bioactive heparin provides a unique feature for use in biocompatible coatings.

Acknowledgment. This study was financially supported by the Promotion Fundamental Studies in Health Science of the Organization for Pharmaceutical Safety and Research (OPSR) under Grant No. 97-15 and in part by a Grant-in-Aid for Scientific Research (A2-12358017, B2-12470277) from the Ministry of Education, Culture, Sports, Science, and Technology of Japan.

LA011408S

Liquid, Phenylazide-End-Capped Copolymers of ϵ-Caprolactone and Trimethylene Carbonate: Preparation, Photocuring Characteristics, and Surface Layering

Manabu Mizutani,† Steven C. Arnold,‡ and Takehisa Matsuda*,§

Department of Bioengineering, National Cardiovascular Center Research Institute, 5-7-1 Fujishiro-dai, Suita, Osaka 565-8565, Japan, Department of Materials Synthesis, Johnson & Johnson Corporate Biomaterials Center, A Division of Ethicon, Inc., Route 22 West, PO Box 151, Somerville, New Jersey 08876-0151, and Department of Biomedical Engineering, Graduate School of Medicine, Kyushu University, 3-1-1 Maidashi, Higashi-ku, Fukuoka 812-8582, Japan

Received November 29, 2001; Revised Manuscript Received April 2, 2002

Photoreactive phenylazide-end-capped liquid copolymers were prepared by ring-opening copolymerization of ϵ-caprolactone (CL) and trimethylene carbonate (TMC) at an equimolar monomer feed ratio in the presence of a polyol, namely, a low-molecular-weight alcohol (di-, tri-, and tetraol) or poly(ethylene glycol) (PEG) as an initiator and tin(II) 2-ethylhexanoate as a catalyst, followed subsequently by phenylazide derivatization at their hydroxyl terminus. These tri- and tetrabranched liquid copolymers (precursors) with a molecular weight from approximately 2500 to 7000 g/mol were cross-linked to yield insoluble solids by ultraviolet (UV) light irradiation. The photocuring rate increased with increasing functionality of phenylazide and UV intensity and decreasing thickness of the liquid film of precursors. The photo-cross-linkability of phenylazide-derivatized liquid copolymers was found to be higher than that of the corresponding coumarin-derivatized liquid copolymers. Poly(lactide) (PLA) films surface-layered with photocured copolymers were prepared by coating surfaces with phenylazide-derivatized copolymers and their subsequent photoirradiation. Endothelial cells adhered well on the nontreated PLA and low-molecular-weight alcohol-based copolymer-layered and photocured films. Little cell adhesion was observed on the hydrolytically surface-eroded PLA film and the PEG-based copolymer-layered film. When a phenylazide-derivatized hexapeptide with the cell-adhesion tripeptidyl sequence, Arg-Gly-Asp (RGD), common to cell adhesive proteins, was photoimmobilized on these surfaces, the surfaces became cell adhesive. Microarchitectured surfaces, which were prepared by sequential procedures of surface coating and photocuring using a photomask with lattice windows, produced regionally differentiated cell adhesiveness.

Introduction

The development of truly blood- or tissue-contacting surfaces of implant devices has been long awaited. To this end, we have been extensively investigating photochemically driven surface modification techniques applicable to the polymeric substrates of biomedical devices.[1−3] The photochemistry reactions utilized can be divided into two different types of reactions, namely, photodimerization reactions, e.g., those of cinnamate,[4] coumarin,[5] and thymine,[6] and photolysis-driven radical generation reactions, e.g., those of phenylazide,[7] dithiocarbamate,[8] benzophenone,[9] and camphorquinone.[10] By use of these reactions, surface derivatization, grafting, and graft polymerization are achieved with high dimensional and regional precision.

On the other hand, for microarchitectural surfaces and device designs, photocurable liquid (co)polymers may be needed, since photoreaction proceeds only at the irradiated portion during irradiation, and liquid-to-solid transformation enables three-dimensional (3D) shaping. That is, liquid biodegradable polymers transformed from a liquid to a solid state and fixed on the substrate surface by photoirradiation may find versatile biomedical applications, such as in biodegradable templates, shape-defined scaffolds, or drug-releasing matrixes, which can essentially be controlled. Such photoprocessing using liquid polymers has the important advantage of not requiring a removal process of unreacted materials thermally induced compared with various techniques including chemical reactions (thermosetting) or other cross-linking reactions. This benefit assumes significance when costly bioactive substances are used.

Copolymers composed of ϵ-caprolactone (CL) and trimethylene carbonate (TMC) within a limited copolymer composition are liquid.[11] Therefore, liquid biodegradable copolymers can be chemically modified at their terminal ends to provide add-on functionality. In our previous report, photocurable and biodegradable liquid copolymer of CL and TMC, in which the coumarin group was endcapped at the molecular termini as the photoreactive center, were synthe-

* To whom all correspondence should be addressed. Telephone: (+81) 92-642-6210. Fax: (+81) 92-642-6212. E-mail: matsuda@med.kyushu-u.ac.jp.
† National Cardiovascular Center Research Institute.
‡ Johnson & Johnson Corporate Biomaterials Center.
§ Kyushu University.

10.1021/bm0101670 CCC: $22.00
Published on Web 05/16/2002

Scheme 1. Photochemical Reactions of Phenylazide upon Ultraviolet Irradiation, Including Chain Extension, Cross-Linking, and Surface Fixation

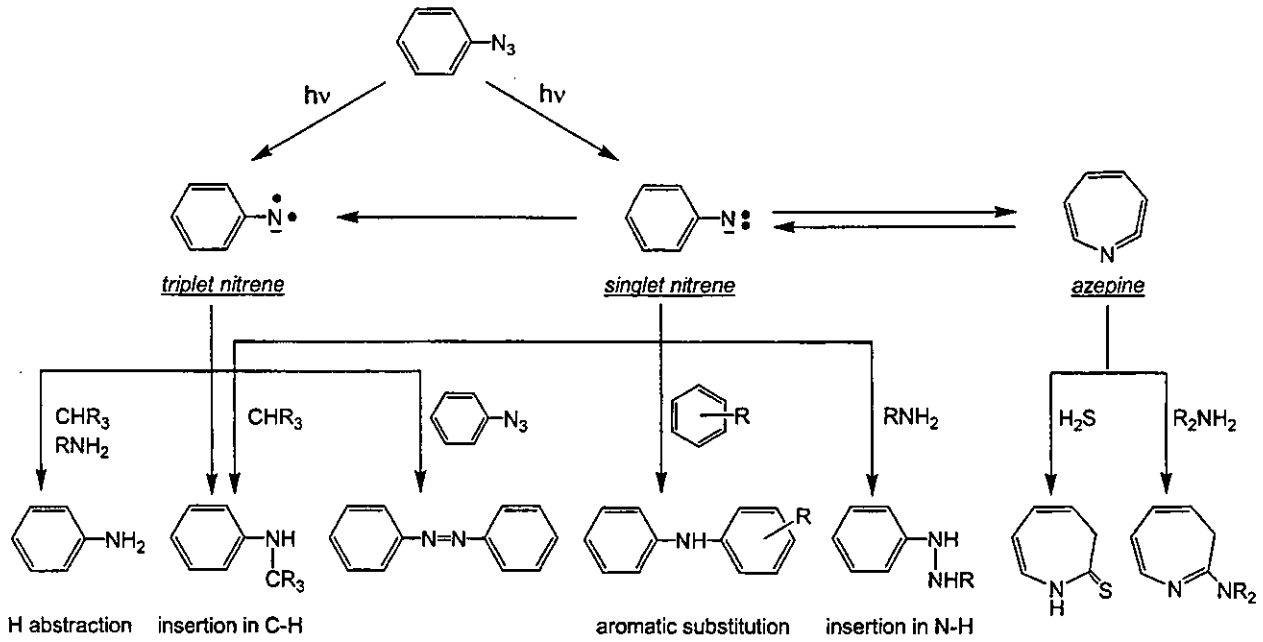

sized, and the photocuring characteristics and preparation of the stereolithographically microprocessed surfaces were described.[12] Intra- and intermolecular dimerization reactions between an associated pair of coumarin groups proceeded with chain extension as well as cross-linking, resulting in the formation of insoluble solids.

In this study, we prepare phenylazide-endcapped liquid copolymers composed of CL and TMC monomer units. Our previous study showed that nitrene, a radical, photolyzed from phenylazide, as schematically shown in Scheme 1,[7b,13] undergoes complex reactions resulting in simultaneous cross-linking and surface grafting or derivatization. It is assumed that the nitrene, a highly reactive radical species, is involved in effective cross-linking and surface fixation. The photocuring rates of phenylazide-derivatized liquid copolymers are compared with those of the corresponding coumarin-derivatized ones. The difference in cell adhesiveness between the copolymers, which were coated on poly(lactic acid) (PLA) films and subsequently photocured, was demonstrated. In addition, regionally differentiated cell adhesive layers were produced by photocuring using photomasks.

Experimental Section

General Procedure. All of the solvents and reagents were purchased from Wako Pure Chemical Industries, Ltd. (Osaka, Japan), or Sigma-Aldrich Japan, Inc. (Tokyo, Japan). Diglycerol polyoxyethylene glycol ether (b-PEG) was obtained from Shearwater Polymers, Inc. (Alabama, USA). TMC was prepared according to a previously reported method,[11] and recrystallized from a mixed solvent of ethyl acetate and hexane. Trimethylolpropane and pentaerythritol were recrystallized from acetone. Other solvents and reagents employed were purified by distillation. PLA films were donated by Johnson & Johnson Corporate Biomaterials Center (New Jersey, USA), and poly(ethylene terephthalate) (PET) films were purchased from Wako Pure Chemical Industries, Ltd. (Osaka, Japan). ^{1}H NMR spectra were recorded on a JEOL JNM-GX270 FT-NMR spectrometer (270 MHz, Tokyo, Japan). The chemical shifts were given as δ values from Me_4-Si as the internal standard. IR spectra were recorded on a Shimadzu DR-8020 FT-IR spectrophotometer (Kyoto, Japan). UV absorption spectra were recorded on a JASCO Ubest-30 UV/VIS spectrophotometer (Tokyo, Japan). The chemical composition of the outermost surface layer was determined by X-ray photoelectroscopy (ESCA-3400, Shimadzu, Kyoto, Japan). The molecular weights of the polymers were determined by gel permeation chromatography (GPC) analysis, which was carried out using a Toso SC-8020 (Tokyo, Japan). The standard molecular weights of PEO (poly(ethylene oxide)) were used as calibration, UV irradiation was carried out on a Hamamatsu Photonics L5662-02 (250 W mercury−xenon (Hg−Xe) lamp, Shizuoka, Japan). The intensity of the UV light source was measured at 250 nm on a TOPCON UVR-25 (Tokyo, Japan). The surface topographic changes were determined by scanning electron microscopy (SEM; JEOL JSM-6301F, Tokyo, Japan).

Synthesis of Poly(ϵ-caprolactone-*co*-trimethylene carbonate) Copolymer (Poly(CL/TMC)). The preparation of the poly(CL/TMC)s was carried out according to a previously reported method.[12] Briefly, a reaction mixture of 0.33 M tin-(II) 2-ethylhexanoate solution in toluene (125 μL, 43 μmol), trimethylene glycol (7.36 g, 96.7 mmol), TMC (64.0 g, 627 mmol), and CL (71.8 g, 629 mmol) was stirred for 8 h at 180 °C in N_2 atmosphere. After vacuum distillation of the unreacted monomers, liquid copolymer, poly(CL/TMC) (**2a**), was isolated by precipitation in methanol. The yield was 139.0 g (99%). Number average molecular weight (M_n) = 2.2 × 10^3 g/mol (determined by GPC; eluent, DMF). FT-IR

Table 1. Liquid Copolymers Based on CL and TMC

copolymer code name	initiator[a] R(OH)$_n$	n[b]	nonendcapped copolymer: copolymer composition CL:TMC[c]	nonendcapped copolymer: M_n[d]	nonendcapped copolymer: M_w/M_n[h]	endcapped copolymer: phenylazide content[e]	endcapped copolymer: phenylazide M_w[f]	endcapped copolymer: coumarin content[e]	endcapped copolymer: coumarin M_w[f]
2a	$CH_2(CH_2OH)_2$	2	0.50:0.50	2.2×10^3	1.2	7.73×10^{-4}	2.6×10^3		
2b	PEG1000	2	0.52:0.48	3.3×10^3	1.2	5.70×10^{-4}	3.5×10^3		
3	$CH_3CH_2C(CH_2OH)_3$	2	0.51:0.49	3.5×10^3	1.3	7.66×10^{-4}	3.9×10^3	8.10×10^{-4}	3.7×10^3
4a	$C(CH_2OH)_4$	2	0.49:0.51	5.1×10^3	1.4	7.65×10^{-4}	5.2×10^3	7.90×10^{-4}	5.1×10^3
4b	b-PEG[g]	2	0.49:0.51	7.2×10^3	1.4	5.71×10^{-4}	7.0×10^3		

[a] Molar fraction of monomer per OH groups was fixed at 6.6. [b] Multifunctionality of the initiator. [c] Copolymer composition of CL/TMC determined by ^{1}H NMR spectroscopy. [d] Number-average molecular weight determined by GPC (PEO standard). [e] Phenylazide or coumarin content calculated by UV spectroscopy (mol/g). [f] Molecular weight (M_w) calculated from the phenylazide or coumarin content. [g] Diglycerol polyoxyethylene glycol ether (mol wt 2040) purchased from Shearwater, Inc. [h] Polydispersity index: M_w/M_n (determined by GPC where M_w is weight-average molecular weight).

(KBr, cm^{-1}): 3529, 2955, 2866, 1744, 1252, 1164, and 1036. ^{1}H NMR (270 MHz, $CDCl_3$, ppm): δ = 1.37 (multiplet), 1.62 (multiplet), 2.01 (multiplet), 2.27 (multiplet), 3.68 (multiplet), and 4.20 (multiplet).

Synthesis of Phenylazide-Endcapped Poly(CL/TMC). The typical procedure for the synthesis of phenylazide-endcapped poly(CL/TMC) was as follows. A mixture of (**2a**) (8.50 g, 3.4 mmol) and 4-azidobenzoyl chloride (2.50 g, 13.8 mmol) was stirred for 12 h at 40 °C in N_2 atmosphere. The reaction was monitored by UV spectroscopy. The resulting liquid phenylazide-endcapped copolymer of (**2a**) was isolated and purified by removal of hydrochloric acid and unreacted 4-azidobenzoyl chloride under reduced pressure and by subsequent precipitation in methanol, respectively.

The content phenylazide of the copolymer was 7.73×10^{-4} mol/g. On the basis of this value, the molecular weight was calculated to be 2.6×10^3 g/mol as follows. The phenylazide content of the grafted copolymer (number of coumarin per weight) was spectroscopically determined in 1,4-dioxane solution using an ϵ_{max} of 2.20×10^4 (271 nm). The molecular weight of grafted copolymer was calculated by multiplying the inverse of the phenylazide content of the photoreactive group by the number of graft chains per molecule (Table 1). ^{1}H NMR (270 MHz, $CDCl_3$, ppm): δ = 1.37 (multiplet), 1.62 (multiplet), 2.01 (multiplet), 2.27 (multiplet), 4.20 (multiplet), 7.05 (doublet, J = 8.1 Hz), and 8.01 (doublet, J = 8.1 Hz).

Synthesis of Coumarin-Endcapped Poly(CL/TMC). Coumarin-endcapped poly(CL/TMC) was synthesized by esterification of the terminal ends of poly(CL/TMC) with coumarin chloride, according to our previously reported method.[12]

Synthesis of Phenylazide-Derivatized Hexapeptide. The hexapeptide, Gly-Arg-Gly-Asp-Ser-Pro (GRGDSP), synthesized in our previous study, was reacted with 4-azidobenzoyloxysuccinimide to yield the photoreactive hexapeptide according to the method described in our previous report.[15]

Photocuring Characteristics. Each phenylazide-endcapped copolymer was coated on a coverglass (15 mm diameter) with dichloromethane solution, and the coverglass was subsequently air-dried and UV-irradiated using a Hg–Xe lamp (250–420 nm). After the coverglass was immersed in dichloromethane solution overnight, the insoluble copolymer was weighed. The photocuring yield was defined as the weight percentage of the insoluble part (W_g) relative to that of the coated copolymer (W): $W_g/W \times 100$.

Surface Layering on PLA Films. Phenylazide-endcapped copolymers were coated onto PLA films by a spin-coater (Mikasa Spinner 1H-DX2, Tokyo, Japan). After UV irradiation for 1 min at 50 mW/cm^2, the films were thoroughly washed with 2-propanol.

Photoreactive Hexapeptide-Immobilized on PLA Film. Photochemical immobilization of the photoreactive hexapeptide was carried out according to the method described in our previous report.[13] Briefly, the photoreactive hexapeptide was dissolved in methanol/deionized water (5/2 v/v, hexapeptide concentration 0.5 wt %) and spread on the PLA film. The surface was UV-irradiated for 30 s at an intensity of 50 mW/cm^2 and thoroughly washed with methanol. (Note that little surface oxidation occurred in this irradiation condition.)

Preparation of the Microarchitectured Surface. Phenylazide-endcapped copolymers were coated on PLA films by a spin-coater. After a metallic photomask with a lattice window (dimensions of the lattice, 200 × 200 μm^2) was placed on the film, the surface was UV-irradiated for 1 min at 50 mW/cm^2, and then the films were thoroughly washed with 2-propanol. Repeated cycles using different phenylazide-endcapped copolymers at different regions produced three regionally different photocured regions. Honeycomb-patterned photocured copolymers on PLA substrate were prepared using a metallic honeycomb-type photomask.

Surface Wettability. Static advancing and receding contact angles with deionized water were measured with a contact angle meter (Kyowa Interface Co. Ltd., Tokyo, Japan) at 25 °C by the sessile drop method.

Cell Culture. The prepared surface-modified films (15 mm diameter) and hydrolytically surface-eroded films, which were immersed in an aqueous 0.05 M Tris (tris[(hydroxymethyl)aminomethane]-tris[(hydroxymethyl)aminomethane hydrochloride]) buffer solution (pH 8.0) for 60 h, were washed with ethanol, air-dried, and placed on the bottom of a 24-well tissue culture dish (Corning, NY). Bovine endothelial cells (ECs, 4×10^4 cells/well), harvested from a thoracic artery by collagenaze enzymatic digestion technique, were cultured on the films in Dulbecco's modified Eagle's medium (DMEM; Flow Laboratories, McLean, VA) supplemented with 15% fetal bovine serum (Hyclone Laboratories, Inc., Logen, UT) at 37 °C in an incubator equilibrated with 5% CO_2–95% air.

A) Photoreactive, liquid poly(CL/TMC)

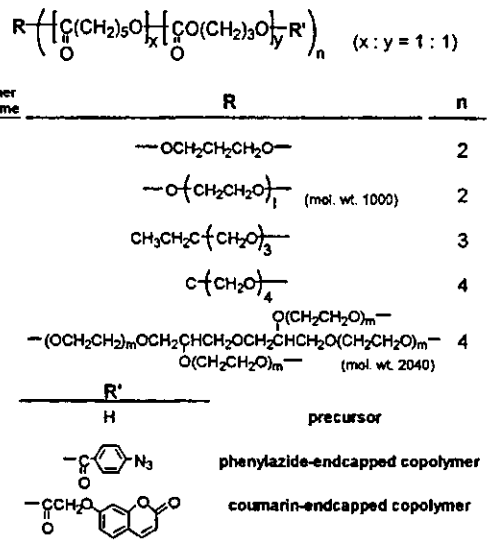

B) Phenylazide-derivatized hexapeptide

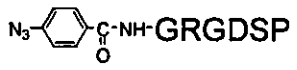

(G: Gly, R: Arg, D: Asp, S: Ser, P: Pro)

Figure 1. Poly(CL/TMC)s and their photoreactive derivatives (A) and phenylazide-derivatized cell adhesive hexapeptide (B).

Results

Preparation of the Phenylazide-Endcapped Poly(CL/TMC) Copolymers. The phenylazide-endcapped copolymers, poly(CL/TMC)s, shown in Figure 1, were prepared by a two-step reaction according to our previously reported method.[12] First, the ring-opening copolymerization of CL and TMC in the presence of a di-, tri-, or tetrafunctional low-molecular-weight alcohol (trimethylene glycol, trimethylolpropane or pentaerythritol, respectively), linear poly(ethylene glycol) (PEG), or a four-branched PEG derivative (b-PEG) as the initiator was carried out at an equimolar feed ratio of CL and TMC. The molar ratio of the monomer to the hydroxyl groups of the initiator was fixed at 6.6, and the reaction was allowed to proceed until completion (almost 100% yield). The compositions of all of the copolymers thus prepared were almost equimolar as expected, as determined by ^{1}H NMR spectroscopy (Table 1). All of the resulting copolymers were viscous liquids. Second, esterification was carried out in the presence of an excess amount of 4-azidobenzoyl chloride against the hydroxyl group, so as to achieve full esterification, which was confirmed by IR and ^{1}H NMR spectroscopies. The phenylazide contents, which were determined by UV spectroscopy, are listed in Table 1.

Photocuring Characteristics. The determination of the photochemical characteristics of liquid films of phenylazide-endcapped copolymers was carried out by UV irradiation. The photocured copolymers, derived from linear copolymers (**2a** and **2b**), initiated with a dialcohol, namely, trimethylene glycol or linear PEG, were soluble in dichloromethane. On the other hand, tri- and tetrafunctionalized phenylazide-endcapped copolymers produced cross-linked copolymers

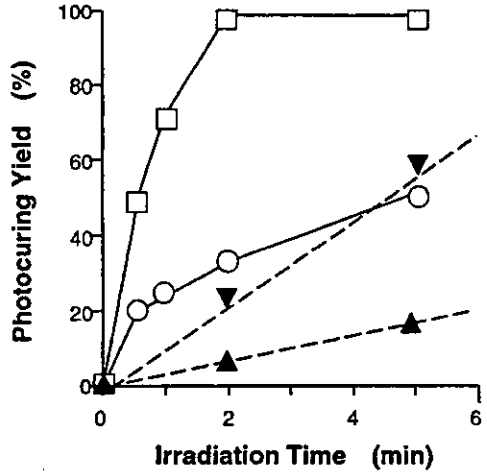

Figure 2. Time-dependent photocuring yield of copolymers: tribranched phenylazide-endcapped (**3**) (○); tribranched coumarin-endcapped (**3**) (▲); tetrabranched phenylazide-endcapped (**4a**) (□); and tetrabranched coumarin-endcapped (**4a**) (▼) copolymers; liquid-film thickness, 0.03 mm; UV intensity, 10.8 mW/cm^2.

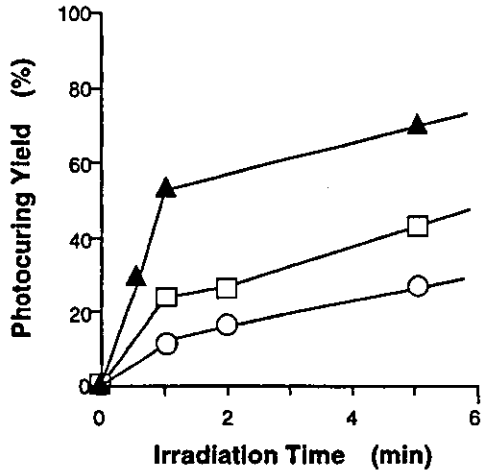

Figure 3. Time-dependent photocuring yield of copolymer (**3**) at various thicknesses: liquid-film thicknesses, 0.03 mm (▲), 0.10 mm (□), and 0.20 mm (○); UV intensity, 100 mW/cm^2.

that were not soluble in any organic solvent. The photocuring yield (nonsoluble part of a photocured copolymer) increased with the photoirradiation time (Figure 2). Tetrabranched copolymers exhibited photocuring characteristics superior to those of tribranched ones. The photocuring rate of phenylazide-endcapped copolymers was much higher than that of the corresponding coumarin-endcapped copolymers (data previously reported[11a] and incorporated in Figure 2). As shown in Figure 3, a higher photocuring yield was obtained with a thinner liquid film (0.03 mm thickness) than with thicker ones (0.10 and 0.20 mm). The UV-intensity dependence of photocuring is shown in Figure 4A. The photocuring yield increased with UV light intensity in the range of 0.5–20 mW/cm^2; however, the intensity dependence appeared to level off at more than 20 mW/cm^2. Little dependence was observed at higher intensities (50 or 100 mW/cm^2). As shown in Figure 4B, the initial photocuring rate, determined from the slope during the early period of photoirradiation in Figure 4A, increased with the UV light intensity. A very high

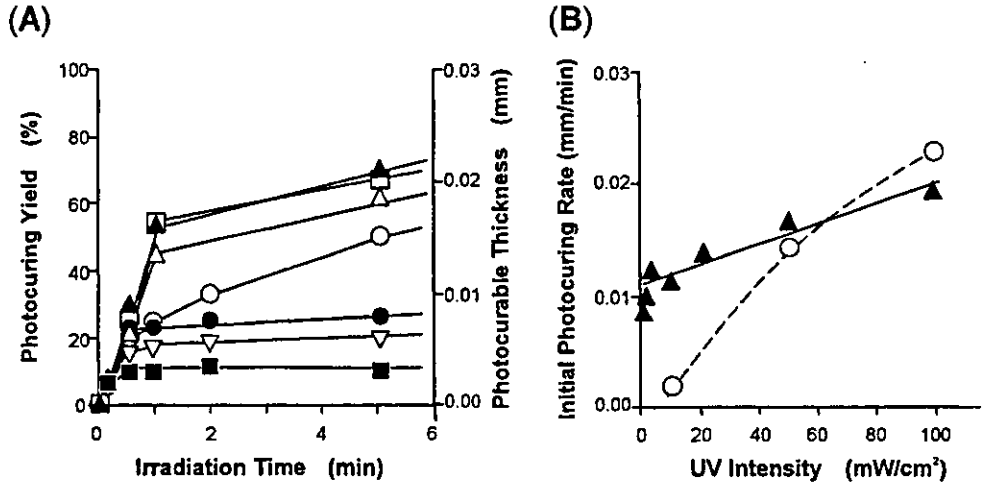

Figure 4. (A) Time-dependent photocuring yield of phenylazide-endcapped copolymers (**3**) at various UV intensities: film thickness, 0.03 mm; UV intensities, 0.5 (■), 1.0 (▽), 2.0 (●), 10 (○), 20 (△), 50 (□), and 100 (▲) mW/cm². (B) Photocuring rate of tribranched copolymers (**3**) (phenylazide-endcapped (▲) and coumarin-endcapped (○) copolymers): liquid film thickness, 0.03 mm.

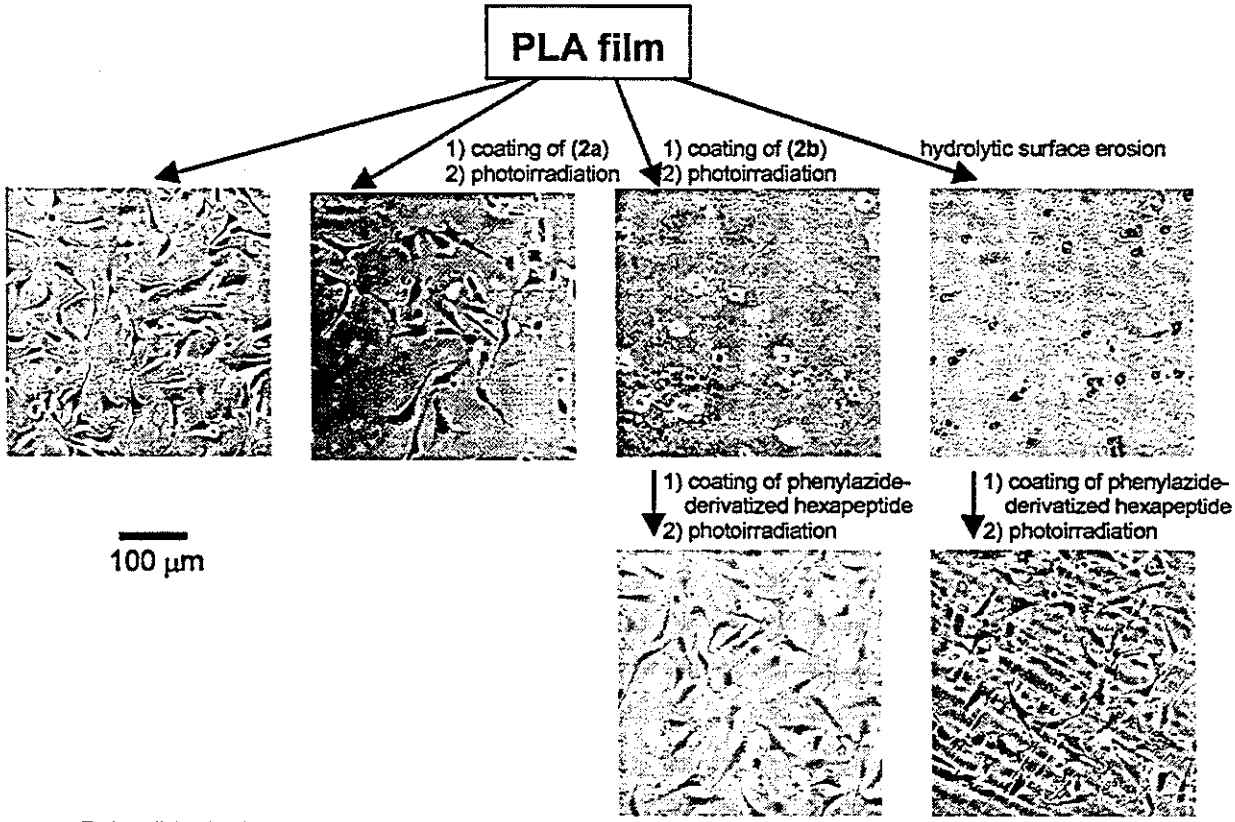

Figure 5. Endothelial cell adhesion behavior on a nontreated poly(lactide) (PLA) film (left, upper), photocured copolymer (**2a** or **2b**)-layered PLA films (intermediate, upper), hydrolytically surface-eroded PLA film (right, upper), and cell-adhesive peptide-photoimmobilized surfaces (lower) on noncell adhesive surfaces.

photocuring rate at low intensities, followed by its gradual increase at higher intensities, was observed. This is in marked contrast with the case of coumarin-endcapped copolymers, in which the photocuring rate increased proportionally with UV light intensity over the entire range of light intensity employed in this experiment (Figure 4B). This may be derived from the difference in the intensity-dependent efficacy of photolysis of phenylazide and photodimerization of coumain groups, suggesting that the efficacy of photolysis of phenylazide is very high and appeared to saturate at relatively low intensity.

Surface Wettability of the Photocured Phenylazide-Endcapped Copolymers on PLA Films. Phenylazide-endcapped copolymers were thinly coated, UV irradiated for 1 min, and then thoroughly washed with 2-propanol. As shown in Table 2, the water receding contact angle of the photocured film was 32° for the copolymer (**2a**) and less than 5° for PEG-based copolymers (**2b** and **4b**). After a 60-h

Table 2. Water Contact Angle of a Phenylazide-Endcapped Copolymer-Coated PLA Film

surface	water contact angle (deg)[a] advancing	receding
PLA (substrate)	72	51
(**2a**)-coated PLA[b]	70	32
(**2b**)-coated PLA[b]	60	<5
(**4b**)-coated PLA[b]	60	<5
immersed PLA[c]	54	<5

[a] Measured by the sessile drop method. Experimental error: ±5%. [b] Coated thickness: 0.01 mm. [c] PLA file immersed in pH 8.0 Tris buffer aqueous solution for 60 h.

immersion in Tris-buffered solution (pH 8.0), the PLA surface exhibited a low receding contact angle (Table 2). These results indicate that PEG-based copolymers and alkali-treated PLA surfaces were very hydrophilic.

Cell Culture on the Surface-Layered PLA Films. Endothelial cells (ECs) adhered and spread well on non-treated PLA films and photocured copolymer (**2a**)-layered PLA films. On the other hand, little cell adherence was observed on photocured PEG-based copolymer (**2b** and **4b**)-layered PLA films and hydrolytically surface-eroded PLA films, which were subjected to a 60-h immersion in Tris-buffered solution (pH 8.0) (Figure 5). Following surface photoimmobilization of the photoreactive hexapeptide peptide with the Arg-Gly-Asp (RGD) tripeptide sequence on these non-cell-adhesive surfaces, which was carried out by solution casting of the photoreactive peptide followed by UV irradiation,[14] X-ray photoelectron spectroscopic observations showed that, upon photoimmobilization, the elemental ratio of nitrogen to carbon at the outermost layers increased drastically, and the water wettability was enhanced (data not shown). Cells adhered and grew well on such surfaces (Figure 5).

Regional Differentiative Cell Adhesiveness. The copolymer **2a** or **2b** was thinly coated on PLA films and photoirradiated by shielding the nonphotocured region using a metallic photomask. After thorough washing with 2-propanol, coating at a different region, photoirradiation, and washing were sequentially performed, to yield three regions with different surface coatings: noncoated, copolymer (**2a**)-coated and copolymer (**2b**)-coated regions. Upon EC seeding, different degrees of cell adhesion and spreading, depending on the surface characteristics, were regionally noted. Good adhesion and spreading were observed in the first two regions, whereas a marked reduction in both cell adhesion and spreading was observed on the copolymer (**2b**)-coated surface (Figure 6). Different degrees of adhesiveness between the hydrophilic PEG-based copolymers (**2b** and **4b**) were demonstrated for honeycomb-like micropatterned PLA films prepared by coating and subsequent photoirradiation using a honeycomb-patterned photomask (Figure 7). After thorough washing, a micropatterned surface, in which the photoirradiated region was photochemically layered with PEG-based copolymer (**2b**) or (**4b**), was prepared (Figure 7). Cell adhesion was observed on the nonirradiated portions, irrespective of the type of PEG-based copolymer coating. On the photoirradiated portions, a fairly reduced adhesion was observed on copolymer (**2b**)-coated regions, and complete

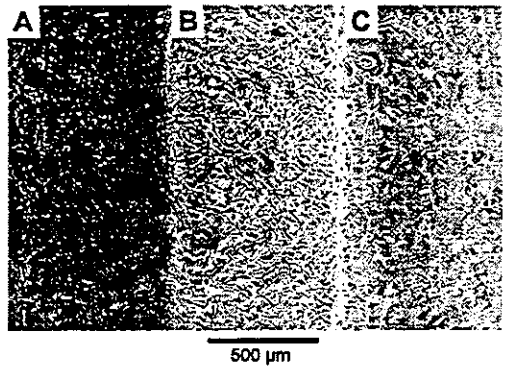

Figure 6. Regionally differentiated cell adhesiveness on three different regions (A, photocured copolymer (**2a**)-layered PLA; B, nontreated PLA; C, photocured copolymer (**2b**)-layered PLA).

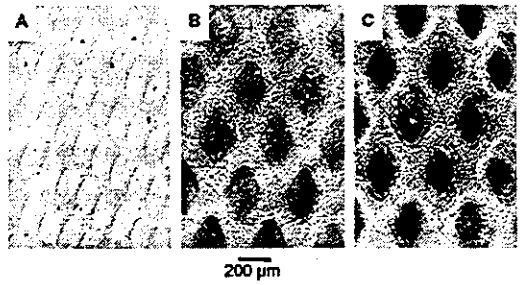

Figure 7. Endothelial cell adhesion on honeycomb-patterned layered surfaces (honeycomb-pattern region, PLA; region inside the pattern, photocured copolymer **2b** or **4b**): A, honeycomb-patterned copolymer (**2b**)-layered PLA surface (before cell seeding); B, endothelial cell adhesion on a honeycomb-patterned copolymer (**2b**)-layered PLA surface; C, endothelial cell on a honeycomb-patterned copolymer (**4b**)-layered PLA surface. Note the reduced adhesion on the copolymer (**2b**)-layered surface and absence of adhesion on the copolymer (**4b**)-layered surface as compared with nontreated PLA honeycomb patterns.

absence of cell adhesion was observed on copolymer (**4b**)-coated surfaces, indicating that a copolymer (**4b**)-coated layer exhibits much higher noncell adhesivity than a copolymer (**2b**)-coated layer.

Discussion

To realize the tissue engineered devices which are truly accepted by body and function as a replacement tissue for diseased or lost tissues, new concept-incorporated extracellular matrix engineering and scaffold engineering[5,6] should be developed. To this end, photochemical process technology may promise new materials and processed devices. Aqueous solutions of photocurable copolymers exhibit solution-to-hydrogel transformation upon photoirradiation, whereas liquid, biodegradable copolymers exhibit liquid-to-solid transformation. Poly(CL/TMC)s are viscous liquid when the compositional ratio of CL to TMC is properly selected.[12] As for liquid biodegradable copolymers, we prepared di-, tri-, and tetrabranched poly(CL/TMC)s at an equimolar ratio. By complete capping of the terminal hydroxyl groups of the poly(CL/TMC)s with a carboxylated coumarin, coumarin-endcapped poly(CL/TMC)s were obtained.[11] Our previous study showed that tri- and tetrafunctional coumarin-endcapped poly(CL/TMC)s underwent liquid-to-solid phase

transformation upon UV irradiation. The photocuring characteristics of these poly(CL/TMC)s such as their dependence on UV light intensity, irradiation time, and thickness were thoroughly studied.[11a,12a]

In this paper, as an extension of our series of studies, phenylazide-endcapped poly(CL/TMC)s were prepared and their photocuring characteristics were studied in comparison with those of coumarin-endcapped ones previously reported by us. The results are summarized as follows.

(1) Increase in the multifunctionality resulted in higher photocuring rates (Figure 2).

(2) The thinner the film, the higher the photocuring rate (Fugure 3).

(3) Much higher UV light intensity dependence of the photocuring rate in low intensity regions was observed for phenylazide-endcapped poly(CL/TMC)s than for coumarin-endcapped ones (Figure 4). This is due to the fact that cross-linking of phenylazides proceeds via radical species, the reaction rate of which is very fast as compared with the photodimerization rate of coumarin groups, which occurs only between an associated pair of coumarin groups.

(4) The hydrophobic copolymer (**2a**) allowed cell adhesion to the same degree as a PLA film, whereas a hydrophilic PEG-based copolymer and **4b**-coated surfaces did not allow cell adhesion (Figure 5).

In general, cell adhesion is mediated by adhesive proteins adsorbed on the surface via ligand−receptor interactions.[15] This suggests that adhesive proteins such as fibronectin, vitronectin, and fibrinogen present in the serum adsorbed onto these hydrophobic surfaces, consequently enhancing both cell adhesion and spreading. In contrast to such a biologically specific mechanism of adhesion, the noncell adhesivity of the hydrophilic PEG-based copolymer layer may involve a physicochemical mechanism; the minimal adsorption of these adhesive proteins as well as the characteristics of easy desorption may be due to the thermodynamic requirement driven by the minimal interfacial free energy change at the water/substrate interface and the structurally diffuse interface structure derived from a water-swollen layer. Such surface-dependent characteristics of protein adsorption and cell adhesion, that is, the difference in the degree of protein adsorptiveness and cell adhesiveness between hydrophobic and hydrophilic surfaces, have been discussed over the years.[16]

(5) The phenylazide-derivatized cell adhesive hexapeptide (GRGDSP), which has the sequence of the cell-adhesion domain of fibronectin (note that the RGD tripeptidyl sequence is the least common sequence of cell-adhesion sites of adhesive proteins[15]) provided a very effective cell adhesive matrix when photoimmobilized (Figure 5). This is in good agreement with the results in our previous study[14] and others.[17]

(6) Surface layering and micropatterning of these copolymers were easily achived by sequential procedures of thin-layer coating, photoirradiation with or without the use of a photomask, and washing. PLA is cell adhesive, but upon being covered with a thin layer of PEG-based copolymer (**4b**), the surface did not allow any cell adhesion (Figure 6), which is due to very hydrophilic nature derived from PEG in the copolymer, resulting in less protein adsorption and easy desorption as typically observed for nonionic hydrophilic polymer.

(7) The different responses of cell adhesiveness of hydrophobic and PEG-based hydrophilic surface layers were clearly observed on micropatterned layered films (Figures 6 and 7).

Thus, phenylazide-derivatized liquid biodegradable copolymers may be used for microarchitectural surface designs and functional surface layering, by which two- or three-dimensional control of biodegradability, as well as the cell and tissue adhesivity, may be precisely manipulated. Since the stereolithographic technique manipulated by computer-assisted design enables microarchitectural photoconstructs, functional tissue engineered devices may be tailored made using these liquid biocompatible materials. In this forthcoming paper, detailed in vivo performances will be reported.[18]

Acknowledgment. M.M. appreciates the financial support from Johnson & Johnson Medical Japan (Tokyo, Japan) and the continuous encouragement of Dr. G. N. Kumar and Dr. A. G. Scopelianos (both of whom are from Johnson & Johnson). This study was financially supported by the Promotion of Fundamental Studies in Health Science of the Organization for Pharmaceutical Safety and Research (OPSR) under Grant No. 97-15, and in part by a Grant-in-Aid for Scientific Research (A2-12358017, B2-12470277) from Ministry of Education, Culture, Sports, Science, and Technology of Japan.

References and Notes

(1) (a) McAuslan, B. R.; Johnson, G. *J. Biomed. Mater. Res.* **1987**, *21*, 921. (b) Yukoshi, T. U.; Matsuda, T. *Langmuir* **1995**, *11*, 4135. (c) Sugawara, T.; Matsuda, T. *J. Biomed. Mater. Res.* **1996**, *32*, 157. (d) Tong, Y. W.; Shoichet, M. S. *J. Biomed. Mater. Res.* **1998**, *42*, 85.

(2) (a) Holland, N. B.; Qiu, Y.; Ruegsegger, M. *Nature* **1998**, *392*, 799. (b) Nakayama, Y.; Miyamura, M.; Hirano, Y.; Goto, K.; Matsuda, T. *Biomaterials* **1999**, *20*, 963.

(3) (a) Nakayama, Y.; Matsuda, T.; Irie, M. *ASAIO J.* **1993**, *39*, M542. (b) Yamamoto, Y.; Sefton, M. V. *J. Biomater. Sci., Polym. Ed.* **1998**, *9*, 427. (c) Lee, H. J.; Matsuda, T. *J. Biomed. Mater. Res.* **1999**, *47*, 564.

(4) (a) Nakayama, Y.; Matsuda, T. *J. Polym. Sci., Part A: Polym. Chem.* **1993**, *31*, 977. (b) Nakayama, Y.; Matsuda, T. *J. Polym. Sci., Part A: Polym. Chem.* **1993**, *31*, 3299.

(5) (a) Matsuda, T.; Moghaddam, M. J.; Miwa, H.; Sakurai, K.; Iida, F. *ASAIO J.* **1992**, *38*, M154. (b) Moghaddam, M. J.; Matsuda, T. *J. Polym. Sci.-Chem. Ed.* **1993**, *A31*, 1589.

(6) Matsuda, T.; Miwa, H.; Moghaddam, M. J.; Iida, F. *ASAIO J.* **1993**, *39*, M327.

(7) (a) Tseng, Y.-C.; Park, K. *J. Biomed. Mater. Res.* **1992**, *26*, 373. (b) Sugawara, T.; Matsuda, T. *Macromolecules* **1994**, *27*, 7809. (c) Ito, Y.; Chen, G.; Guan, Y.; Imanishi, Y. *Langmuir* **1997**, *13*, 2756.

(8) (a) Nakayama, Y.; Matsuda, T. *Macromolecules* **1996**, *29*, 8622. (b) Higashi, J.; Nakayama, Y.; Marchant, R. E.; Matsuda, T. *Langmuir* **1999**, *15*, 2080.

(9) (a) Nakayama, Y.; Ishibashi, K.; Matsuda, T. *Jpn. J. Artif. Organs* **1995**, *24*, 102. (b) Nakayama, Y.; Matsuda, T. *J. Biomed. Mater. Res.* **1999**, *48*, 511.

(10) (a) Meniga, A.; Tarle, Z.; Ristic, M.; Sutalo, J.; Pichler, G. *Biomaterials* **1997**, *18*, 1349. (b) Nakayama, Y.; Matsuda, T. In preparation.

(11) (a) Scopelianos, A. G.; Bezwada R. S.; Arnold, S. C.; Gooding, R. D. US Patent 5,411,554, July, 1993. (b) Scopelianos, A. G.; Arnold, S. C.; Bezwada, R. S.; Roller, M. B.; Huxel, S. T. US Patent 5,-599,852, October, 1994. (c) Bezwada R. S.; Arnold, S. C.; Shalaby,

W. S. US Patent 5,653,992, April, 1995. (d) Scopelianos, A. G.; Arnold, S. C.; Bezwada, R. S.; Roller, M. B.; Huxel, S. T. US Patent 5,728,752, March, 1996. (e) Scopelianos, A. G.; Bezwada, R. S.; Arnold, S. C. US Patent 5,824,333, November, 1996.

(12) (a) Matsuda, T.; Mizutani, M.; Arnold, S. C. *Macromolecules* **2000**, *33*, 795. (b) Matsuda, T.; Mizutani, M. *Macromolecules* **2000**, *33*, 791. (c) Matsuda, T.; Mizutani, M. *Biomacromolecules* **2002**, *3*, 249–255.

(13) Patai, S., Ed. *The Chemistry of Azido Group*; Interscience Publishers: London, 1971.

(14) Sugawara, T.; Matsuda, T. *J. Biomed. Mater. Res.* **1995**, *29*, 1047.

(15) Pierschbacher, M. D.; Rouslahti, E. *Nature* **1984**, *309*, 33.

(16) Kidoaki, S.; Matsuda, T. *Langmuir* **1999**, *15*, 7639.

(17) (a) Massia, S. P.; Hubble, J. A. *Anal. Biochem.* **1990**, *187*, 292. (b) Imanishi, Y.; Ito, L.; Kajiwara, M. *J. Macromol. Sci. Chem.* **1988**, *A45*, 555.

(18) Matsuda, T.; Mizutani, M. *J. Biomed. Mater. Res.*, in press.

BM0101670

Preparation of Vinylated Polysaccharides and Photofabrication of Tubular Scaffolds as Potential Use in Tissue Engineering

Takehisa Matsuda*,† and Tomoko Magoshi‡

Department of Biomedical Engineering, Graduate School of Medicine, Kyushu University, 3-1-1, Maidashi, Higashi-ku, Fukuoka 812-8582, Japan, and Department of Bioengineering, National Cardiovascular Center Research Institute, 5-7-1, Fujishiro-dai, Suita, Osaka 565-8565, Japan

Received February 21, 2002; Revised Manuscript Received June 3, 2002

Polysaccharides, such as heparin, hyaluronan, and chitosan, were partially derivatized with a styryl or a methacryloyl group by condensation at a carboxyl or an amino group of the polysaccharides with 4-vinylaniline or 4-vinylbenzoic acid. The degree of substitution depended on the reaction conditions. These compounds with low degrees of derivatization produced water-swollen hydrogels only at relatively high concentrations (30−40 wt %) in the presence of a carboxylated camphorquinone upon visible light irradiation. A high degree of derivatization of heparin increased the gel yield and concomitantly reduced the degree of swelling. The copolymerization of these vinylated polysaccharides with styrenated gelatin considerably reduced the degree of swelling. Tubular photoconstructs were prepared by photocopolymerization of vinylated polysaccharide and vinylated gelatin. The mixing of diacrylated poly(ethylene glycol) with vinylated polysaccharide improved the burst strength of photogels against the gradual infusion of water. These photocurable polysaccharides may be used as photocured scaffolds in tissue-engineered devices.

Introduction

The repair of diseased or lost tissues requires enhanced tissue regeneration or a tissue equivalent for defective tissues. Tissues are composed of cells and extracellular matrix (ECM) that includes collagen, elastin, and proteoglycans. These ECM components extracted in vitro are often soluble in water. However, these are self-organized themselves to produce insoluble supramolecular assemblies or gels in living tissues. Therefore, if such a biomacromolecule is intended for use as artificial ECM, the sol-to-gel phase transformation of these biomacromolecules is essential, which enables the realization of wound healing and cell-incorporated tissue engineering.[1−3] To this end, various chemical or physical gelation techniques have been developed. The authors have been extensively developing photochemically driven gelation technology of biomacromolecules that are chemically modified with photodimerizable groups such as cinnamate[4] and coumarin,[5] photoinduced radical generating groups such as phenyl azide,[6] benzophenone,[7] and dithiocarbamate,[7] and photopolymerizable vinyl groups such as styryl and methacryloyl group.[8,9] Other reaearch groups have been extensively developing photopolymerization of vinylated water-soluble synthetic polymers or polysaccharides for cell-inoculated scaffolds in tissue-engineering and drug-immobilized matrixes. For example, multiply methacrylated polysaccharides including dextran−methacylate,[10] hyaluronate−methacrylate,[14] and alginate−methacrylate[14] have been developed by a few research groups. As photopolymerizable and biodegradable poly(ethylene glycol)-based macromers, acrylated poly(ethylene glycol) derivatives including poly(ethylene glycol)-*co*-poly(α-hydroxy acid) diacrylate[15] and poly(ethylene glycol)-poly(lysine) diacrylate,[16] both of which are end-capped with acryloyl groups, have been studied in detail.

In this study, as an extension of our study on visible-light-induced polymerizable proteins such as vinylated gelatin and vinylated albumin, which were already reported in our previous paper,[8] vinylated polysaccharides including heparin, hyaluronan, and chitosan were newly prepared. As schematically shown in Figure 1, these vinylated polysaccharides were prepared via a condensation reaction of a carboxyl or an amino group of the polysaccharides with a vinyl monomer in the presence of a water-soluble condensation agent. Their gels were prepared by polymerization of the vinylated polysaccharides or copolymerization with vinylated protein mentioned above. In the presence of water-soluble camphorquinone as a photocleavable radical producing agent and under visible light irradiation, aqueous solutions of these vinylated biomolecules were converted to hydrogels. In addition, photocuring characteristics of vinylated polysaccharides were studied, and the photofabrication of tubular constructs derived only from biomacromolecules was demonstrated, which may be useful as a scaffold or a template in tissue-engineered devices.

Experimental Section

Reagents. Gelatin (mol wt 9.5×10^4 g/mol, from bovine bone), heparin sodium salt (198.6 IU/mg), and chitosan (water soluble, mol wt 3.0×10^3 g/mol) were obtained from

* To whom correspondence may be addressed. E-mail: matsuda@med.kyushu-u.ac.jp.
† Kyushu University.
‡ National Cardiovascular Center Research Institute.

10.1021/bm0200229 CCC: $22.00
Published on Web 08/17/2002

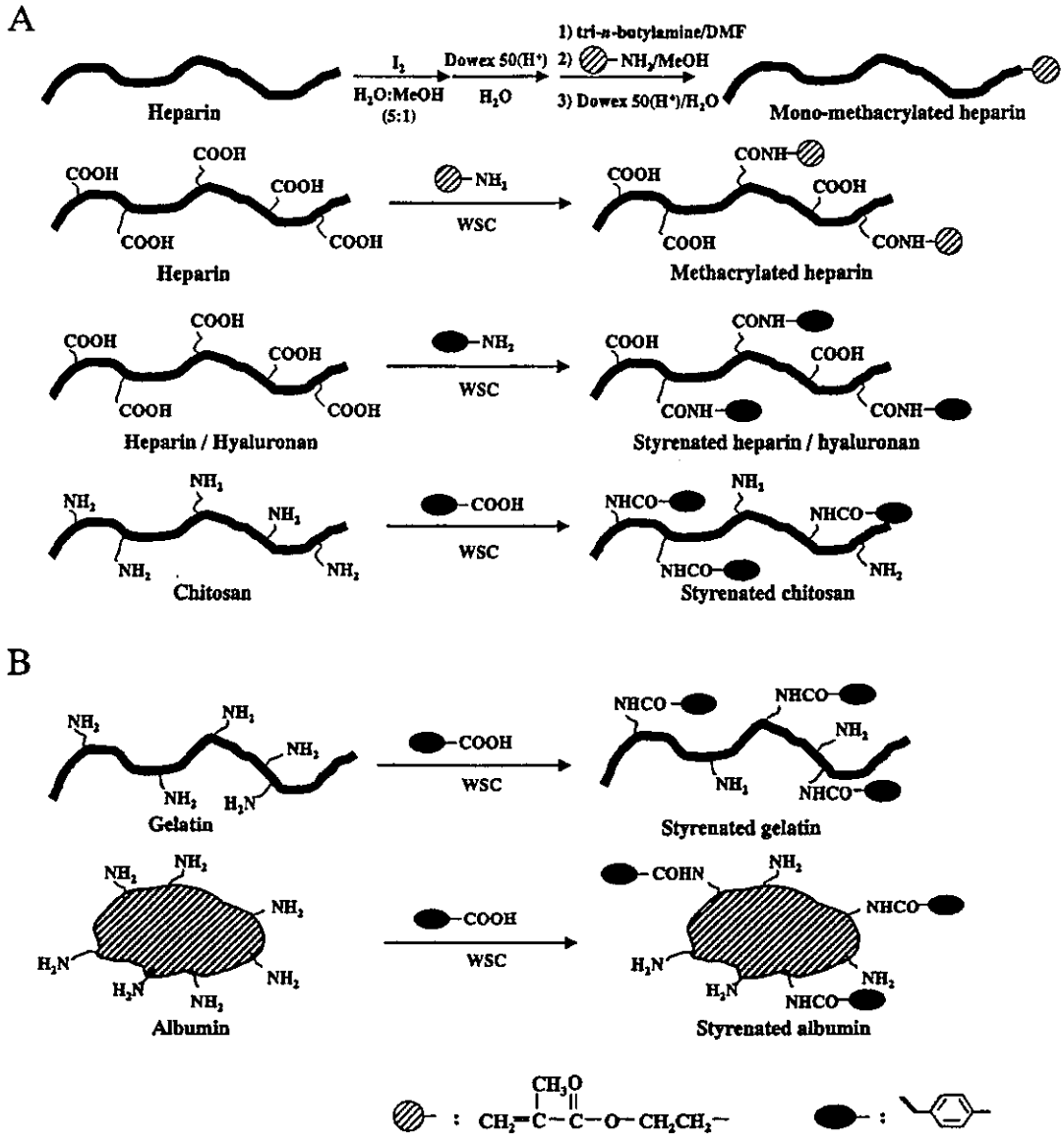

Figure 1. Preparative routes for vinlylated biomacromolecules: (A) polysaccharides including heparin, hyaluronan, and chitosan; (B) proteins including gelatin and albumin.

Wako Pure Chemicals Inc. (Osaka, Japan). Albumin (mol wt 6.6×10^4 g/mol, bovine serum) was obtained from Sigma Chemical Co. (St. Louis, MO). 1-Ethyl-3-(dimethylaminopropyl)carbodiimide hydrochloride (WSC) was obtained from Dojindo Laboratory (Kumamoto, Japan). Sodium hyaluronan (mol wt 3.0×10^5 g/mol) was kindly supplied by Seikagaku Kogyo Co., Ltd. (Tokyo, Japan). 4-Vinylbenzoic acid and 4-vinylaniline were obtained from Tokyo Chemicals Inc., Co., Ltd. (Tokyo, Japan). 2-Aminoethyl methacrylate hydrochloride and poly(ethylene glycol) diacrylates (mol wt 400 g/mol, PEGDA400) were purchased from Polysciences Inc. (PA). Phosphate-buffered saline solution (PBS, pH 7.4) was purchased from Nissui Pharmaceutical Co., Ltd. (Tokyo, Japan).

General Methods. Purification of vinyl-derivatized biomacromolecules was carried out using a dialysis membrane (cut off mol wt = 3×10^3 or 1.2×10^4 to 1.4×10^4, Wako Pure Chemicals Inc., Osaka, Japan). The extensive dialysis against distilled water for 3 days resulted in the complete removal of an unreacted monomer from the solution. ^{1}H NMR spectra were recorded on a JEOL JNM-GX270 FT-NMR spectrometer (270 MHz, Tokyo, Japan). UV−vis spectra were recorded on a Ubest-30 UV−vis spectrophotometer (Japan Spectroscopic Co., Ltd., Tokyo, Japan). Visible light irradiation was carried out with a halogen lamp (Tokuso power light with illumination wavelength, 400−520 nm, Tokuyama Co., Ltd., Yamaguchi and VL-501, LPL Co., Ltd., Tokyo, Japan) and light intensity was measured with a photometer (laser power meter HP-1, Pneum Co., Ltd., Saitama, Japan).

Synthesis of Terminally Methacrylated Heparin. Terminally methacrylated heparin was synthesized by the ring opening addition of the terminal lactone ring of modified heparin with 2-aminoethyl methacrylate. Briefly, heparin was treated with a reducing agent (I_2) to generate a lactone ring at its terminal end (designated as lactone−heparin) according

to our previous method.[17] The lactone−heparin (300 mg, 2.6 × 10^{-5} mol) in *N,N*-dimethylformamide (5 mL) neutralized with tri-*n*-butylamine (1.3 mL) was added to 2-aminoethyl methacrylate hydrochloride (82.8 mg, 5.0 × 10^{-4} mol) in methanol (2 mL), and stirred at 80 °C for 26 h. The reaction mixture was evaporated under reduced pressure. The residue was dissolved in water and passed through a Dowex 50X8 (H^+) column. Extensive dialysis and lyophilization of the eluate gave the terminally methacrylated heparin (285 mg), which was characterized by ^{1}H NMR (D_2O) as follows. The signal intensity of the methyl group of 2-aminoethyl methacrylate appearing at 1.95 ppm relative to the signal intensity of the methyl group of heparin (2.05 ppm) was approximately 0.4, and this remained constant even with prolonged reaction times or at higher concentrations of 2-aminoethyl methacrylate, indicating that terminally methacrylated heparin was produced.

Synthesis of Methacrylated Heparin. To heparin sodium salt (0.50 g, 4.2 × 10^{-5} mol) dissolved in phosphate-buffered saline solution (PBS, pH 7.4), WSC (0.32 g, 1.7 × 10^{-3} mol) was added and stirred at 4 °C for 30 min. Following the addition of 2-aminoethyl methacrylate hydrochloride (1.40 g, 8.3 × 10^{-3} mol) in PBS, the solution was stirred at room temperature for 7 days. The reaction solution was dialyzed and then lyophilized to give the heparin derivative having a methacrylate group as a side chain (0.52 g). The number of derivatized methacrylate groups in a heparin molecule was determined by the titration method as described below. At first, 50 mg of the sample (nonmodified or modified heparin) was dissolved in 20 mL of water. After 0.05 mL of 0.1 N HCl was added to the solution, the solution was titrated dropwise by addition of 0.01 N NaOH under stirring to measure pH. The number of derivatized methacrylate groups was calculated from the difference in the amount of NaOH solution added to the solution to achieve the neutralization point between nonmodified and modified heparin-containing solution.

Synthesis of Styrenated Heparin. Styrenated heparins with different numbers of styrene groups derivatized in a molecule were prepared at various concentrations of 4-vinylaniline in the presence of WSC. The typical protocol is described below. Heparin sodium salt (5.43 g, 4.4 × 10^{-4} mol) was dissolved in PBS. After the addition of WSC (3.40 g, 1.8 × 10^{-2} mol), the reaction mixture was stirred at 4 °C for 30 min. 4-Vinylaniline (1.06 g, 8.9 × 10^{-3} mol) was dissolved in 1 N hydrochloric acid, and its pH was adjusted to 3. These two solutions were mixed and stirred at 4 °C for 24 h. The reaction mixture was dialyzed and then lyophilized to give a styrenated heparin (5.92 g). The number of styryl groups incorporated into heparin (mol wt of 1.2 × 10^4 g/mol) was calculated based on its absorbance (4-vinylaniline at 260 nm; $\epsilon = 2.1 \times 10^4$).

Synthesis of Styrenated Hyaluronan. Sodium hyaluronan (100.0 mg, 3.3 × 10^{-7} mol) was dissolved in PBS (100 mL). After the addition of WSC (101.2 mg, 5.2 × 10^{-4} mol), it was stirred at 4 °C for 30 min. After the pH of the aqueous solution of 4-vinylaniline (157.2 mg, 1.3 × 10^{-3} mol), was adjusted to 3 similarly to that above, these two solutions were mixed and stirred at 4 °C for 24 h. The reaction mixture was dialyzed and then lyophilized to give styrenated hyaluronan (83.1 mg). The number of styryl groups incorporated into hyaluronan was calculated based on its absorbance (4-vinylaniline at 260 nm; $\epsilon = 2.1 \times 10^4$).

Synthesis of Styrenated Chitosan. 4-Vinylbenzoic acid (0.8 g, 5.4 × 10^{-3} mol) was dissolved in 1 N sodium hydroxide solution (1 N, 50 mL) and then neutralized to pH 7.6 with 1 N hydrochloric acid. After the addition of WSC (2.2 g, 1.2 × 10^{-2} mol), the reaction solution was stirred at 4 °C for 30 min and subsequently mixed with chitosan (0.5 g, 1.7 × 10^{-7} mol) dissolved in PBS (50 mL). The reaction mixture was stirred at room temperature for 24 h and then dialyzed and lyophilized to give styrenated chitosan (0.8 g). The number of styryl groups incorporated into one chitosan molecule was calculated based on its absorbance (4-vinylbenzoic acid at 260 nm; $\epsilon = 2.0 \times 10^4$).

Synthesis of Styrenated Gelatin. Styrenated gelatin was synthesized by our previous method.[8] 4-Vinylbenzoic acid (5.7 g, 3.9 × 10^{-2} mol) was dissolved in 1 N sodium hydroxide solution (1 N, 50 mL) and then neutralized to pH 7.6 with 1 N hydrochloric acid. After the addition of WSC (14.8 g, 7.7 × 10^{-2} mol), the reaction solution was stirred at 4 °C for 30 min and subsequently mixed with gelatin (10 g, 1.1 × 10^{-4} mol, total number of amino groups was 36.8 per molecule) dissolved in PBS (500 mL). The reaction mixture was stirred at room temperature for 24 h, and then dialyzed and lyophilized to give styrenated gelatin (12.5 g). The number of styryl groups incorporated into one gelatin molecule was determined using a method similar to that previously mentioned (trinitrobenzene sulfuric acid (TNBS) method[21]).

Synthesis of Styrenated Albumin. Styrenated albumin was synthesized by our previous method.[8] 4-Vinylbenzoic acid (0.4 g, 2.7 × 10^{-3} mol) was dissolved in 1 N sodium hydroxide solution (1 N, 50 mL) and then neutralized to pH 7.6 with 1 N hydrochloric acid. After the addition of WSC (1.0 g, 5.4 × 10^{-3} mol), the reaction solution was stirred at 4 °C for 30 min and mixed with albumin (2.0 g, 3.0 × 10^{-5} mol, total number of amino group was 20.6 per molecule) dissolved in PBS (100 mL). The reaction mixture was stirred at room temperature for 24 h, and then dialyzed and lyophilized to give styrenated albumin (1.8 g). The number of styryl groups incorporated into one albumin molecule was determined similarly to that using a method mentioned above.

Gel Yield and Degree of Swelling. (1*S*)-7,7-Dimethyl-2,3-dioxobicyclo[2.2.1]heptane-1-carboxylic acid (carboxylated camphorquinone, CQ-COOH) was used as a water-soluble radical-producing reagent. Its preparation method was described elsewhere.[18] Photopolymerization of vinyl-derivatized biomolecule was carried out as follows. An aqueous solution of vinyl-derivatized biomolecule (0.1 mL; W_{solid} as the solid) containing 0.5 wt % CQ-COOH was placed on a circular glass coverslip (diameter: 11 mm) and irradiated at the light intensity of 200 mW/cm^2 for a predetermined time. After the reaction, nonreacting substances were removed by immersion in distilled water at 40 °C for 12 h, and then the product was weighed (W_{water}). Subsequently, the gels were vacuum-dried and weighed (W_{gel}). Gel yield (%) was

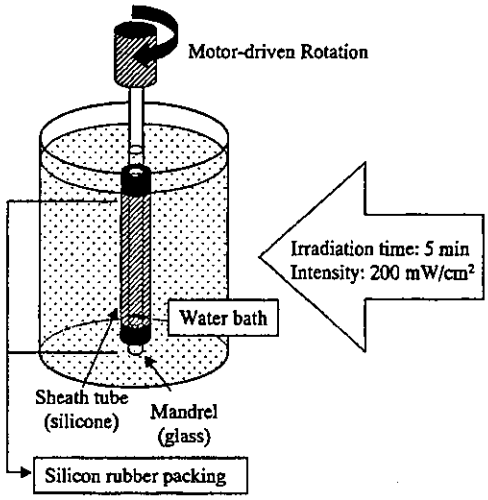

Figure 2. Schematics of the photofabrication of preparation of vinylated polysaccharide-based tubular photoconstruct.

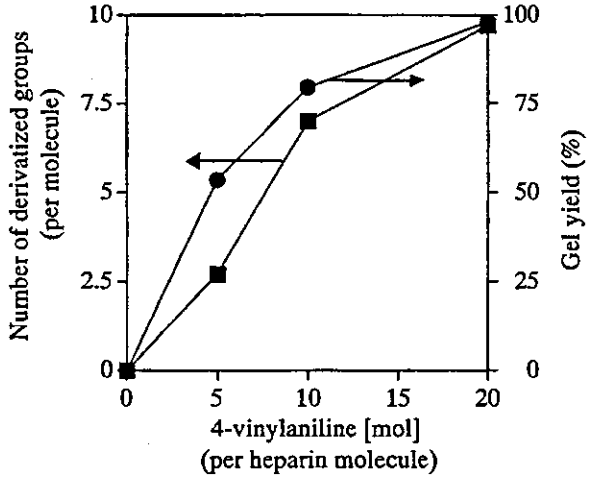

Figure 3. Multiply vinylated heparin prepared by condensation reaction with 4-vinylaniline. The degree of styrene derivatization per heparin molecule and gel yield vs concentration of 4-vinylaniline used in preparation. Gelation conditions: vinylated heparin concentration, 20 wt %; CQ-COOH concentration, 0.5 wt %; 5-min irradiation at 200 mW/cm².

calculated as $W_{gel}/W_{solid} \times 100$. The degree of swelling (DS) was calculated as $DS = (W_{water} - W_{gel})/W_{gel}$.

SEM Observation. The surfaces of photocured films were observed by scanning electron microscopy (SEM) using a JEOL JSM-6301F (Tokyo, Japan) electron microscope. Samples were prepared by either the freeze-drying technique (which was freezing at a predetermined temperature (−20, −70, or −150 °C) for 24 h and then drying under vacuum without melting) or treatment with a graded series of ethanol, critical-point drying followed by plasma-coating with osmium (APC-120, Meiwa Shoji Co. Ltd., Osaka, Japan), and subjecting to SEM observation.

Fabrication of Tubes. An aqueous solution of vinylated biomolecules containing CQ-COOH was poured into the mold: the interspace between the mold was composed of a silicone outer tube (sheath) and a glass inner rod (mandrel), and the mold was immersed into a water bath (Figure 2). Fabrication of tubes employed two kinds of molds: (mold A) diameter of inner rod, 1.4 mm; inner diameter of outer tube, 2.5 mm; tube length, 5 cm; (mold B) diameter of inner rod, 3.0 mm; inner diameter of outer tube, 4.0 mm; tube length 10 cm. Then, these were subsequently photoirradiated with a halogen lamp (200 mW/cm² light intensity, VL-501, LPL Co., Ltd., Tokyo, Japan) for 5 min at 1 revolution/s.

Burst Strength Measurement. The burst strength of the fabricated tubes was determined by continuous infusion of water using a syringe pump (Truth all-round injector, Nakagawa-Seikodo Co., Ltd., Japan; infusion rate, 0.25 mL/min) from one end of the tube in which the other end was sealed by glue. The internal pressure of the tubular segment was measured with a transducer (P10EZ, Gould Statham Instruments Inc., Hato Rey, Puerto Rico), and the external diameter of tubular segment was measured using a cooled coupled digital (CCD) camera (Hamamatsu Photonics K.K., Shizuoka, Japan). A more detailed description is given in our previous paper.[19,20]

Results

Syntheses of Vinylated Biomolecules. Terminally methacrylated heparin was prepared using a procedure reported previously.[17] Briefly, heparin was treated with a reducing agent (I_2) to generate a lactone ring at its terminal end, followed by a ring-opening reaction with 2-aminoethyl methacrylate, which gave terminally monomethacrylated heparin through the formation of an amide group between the terminus of heparin and the monomer (Figure 1A).

Various multiply vinylated biomolecules were prepared by a condensation reaction of carboxyl or amino groups of the side chains of the biomolecules with its counterpart group (amino or carboxyl group) bearing vinyl monomers: carboxyl or amine groups of biomolecules including heparin (mol wt 1.2×10^4 g/mol), hyarulonan (mol wt 3×10^5 g/mol), chitosan (mol wt 3×10^3 g/mol), gelatin (mol wt 9.5×10^4 g/mol), and albumin (mol wt 6.6×10^4 g/mol) with carboxyl or amino groups of vinyl monomers such as 4-vinylbenzoic acid, 4-vinylaniline, and 2-aminoethyl methacrylate. Briefly, these biomolecules were mixed with a vinyl monomer in the presence of WSC as a condensation agent in PBS or water, producing the corresponding vinylated biomolecules. Under certain conditions, heparin was obtained by the coupling reaction of the carboxyl group of the side chain of heparin with 2-aminoethyl methacrylate to produce approximately two methacrylate groups in one molecule (the number of derivatizations per molecule was found be 1.9, which was determined by titration). Styrenated heparins, which were prepared by using 4-vinylaniline at a fixed reaction time but different monomer concentrations, had 2.7, 7.0, and 9.7 styryl groups per heparin molecule (Figure 3). Figure 4 shows the relationship between the initial concentration of 4-vinylaniline and the number of derivatized styryl groups per molecule: An increase in the concentration of 4-vinylaniline in the initial feed almost proportionally increased the number of incorporated styryl groups.

Styrenated hyaluronan was prepared by using 4-vinylaniline, and styrenated gelatin, styrenated chitosan, and styrenated albumin were prepared by using 4-vinylbenzoic acid. Under experimental conditions described in the Experimental Section, the numbers of derivatized styryl groups

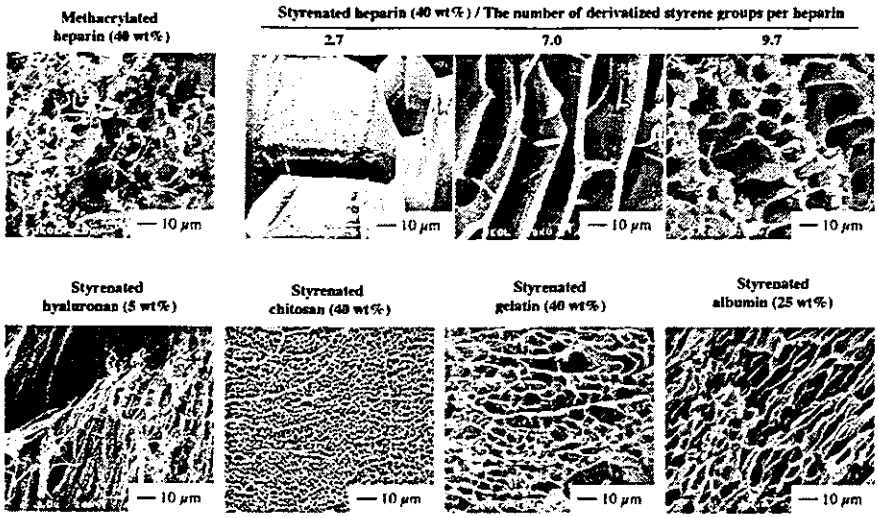

Figure 4. SEM images of freeze-dried photocured vinylated biomacromolecules with different degrees of vinylation at different concentrations.

Table 1. Preparation Conditions for Vinylated Biomolecules and Photocuring Characteristics (Gel Yield and Degree of Swelling)

	coupling reaction (molar ratio)				no. of	visible light irradiation[a]		
biomolecule[b]	function group of biomolecule	vinyl monomer	WSC[c]	reaction time (h)	derivatized groups (per molecule)	concn (wt %)	gel yield (%)	degree of swelling
heparin	terminal-lactone	2-aminoethyl methacrylate 20		26	1.0	40		
heparin	side chain COOH	2-aminoethyl methacrylate 200	40	168	1.9	40	48 ± 3	23 ± 3
heparin	side chain COOH	4-vinylaniline 5	40	24	2.7	40	54 ± 2	28 ± 2
heparin	side chain COOH	4-vinylaniline 10	40	24	7.0	40	79 ± 5	5 ± 0.5
heparin	side chain COOH	4-vinylaniline 20	40	24	9.7	40	98 ± 1	3 ± 0.5
hyaluronan	side chain COOH	4-vinylaniline 40	158	24	24.8	5	91 ± 3	342 ± 100
chitosan	side chain NH_2	4-vinylbenzoic acid 318	706	24	2.9	40	12 ± 1	10 ± 1
gelatin	lysine residue NH_2	4-vinylbenzoic acid 736	1472	24	25.2	40	74 ± 3	12 ± 3
gelatin	lysine residue NH_2	4-vinylbenzoic acid 736	1472	24	40.0	40	84 ± 2	6 ± 1
albumin	lysine residue NH_2	4-vinylbenzoic acid 90	180	24	15.5	25	93 ± 1	7 ± 1

[a] Photointensity, 200 mW/cm^2; photoirradiation time, 5 min; photoinitiator, 0.5 wt % to monomer. [b] Molecular weight of biomolecule (g/mol): heparin, 1.2×10^4; hyaluronan, 3.0×10^5; chitosan, 3.0×10^3; gelatin, 9.5×10^4; albumin, 6.6×10^4. [c] WSC, water soluble carbodiimide, 1-ethyl-3-(dimethylaminopropyl)carbodiimide, hydrochloride.

of styrenated hyaluronan, chitosan, and albumin were 24.8, 2.9, and 15.5 per molecule, respectively. The number of derivatized styryl groups of styrenated gelatins, which were prepared by using a different concentration of 4-vinylbenzoic acid, was 30.0 per molecule. All vinylated biomolecules were soluble in water. Table 1 lists the coupling reaction conditions for the preparation of vinylated biomolecules and the numbers of derivatized vinyl groups per molecule.

Gel Yield and Degree of Swelling. Gel yields and degrees of swelling of hydrogel derived from vinylated biomolecules at a fixed initiator concentration to monomer (0.5 wt %) and at a fixed irradiation condition (5 min and 200 mW/cm^2) are shown in Table 1. For terminally monomethacrylated heparin, the solution became highly viscous upon photoirradiation but little gel was formed because it was only monofunctionalized. On the other hand, aqueous solutions of other vinylated biomolecules formed gels upon irradiation. For styrenated heparin, the gel yield was significantly increased with an increase in the number of derivatized styrene groups, and the degree of swelling in water was concomitantly decreased (Table 1). Other biomolecules were not examined systematically. Very high gel yields and relatively low degrees of swelling were obtained in particular cases of styrenated gelatin and styrenated albumin. Vinylated hyaluronan at a very low concentration (5 wt %) produced a gel with very high degree of swelling at high gel yield.

Since ECMs in the living tissues are composed of different types of biomacromolecules, the authors attempted to produce copolymers of these vinylated biomacromolecules, which may enable manipulation of bioactivity as well as